CHALMERS
UNIVERSITY OF TECHNOLOGY

UNIVERSITY OF GOTHENBURG

Conductivity Measurement of Greywater Using a Microcontroller

with Focus on Cost Reduction

Master's thesis in Department of Computer Science and Engineering

JAKOB NOLKRANTZ

Department of Computer Science and Engineering
CHALMERS UNIVERSITY OF TECHNOLOGY AND UNIVERSITY OF GOTHENBURG
Gothenburg, Sweden 2018

Master's thesis 2018

Conductivity Measurement of Greywater Using a Microcontroller

with Focus on Cost Reduction

Jakob Nolkrantz

Department of Computer Science and Engineering
Chalmers University of Technology and University of Gothenburg
Gothenburg, Sweden 2018

Conductivity Measurement of Greywater Using a Microcontroller
with Focus on Cost Reduction
Jakob Nolkrantz

Supervisor: Roger Johansson, Department of Computer Science and Engineering
Examiner: Per Larsson-Edefors, Department of Computer Science and Engineering

Master's Thesis 2018
Department of Computer Science and Engineering
Chalmers University of Technology and University of Gothenburg
SE-412 96 Gothenburg
Telephone +46 31 772 1000

Typeset in LaTeX
Gothenburg, Sweden 2018

Conductivity Measurement of Greywater Using a Microcontroller
with Focus on Cost Reduction
Jakob Nolkrantz
Department of Computer Science and Engineering
Chalmers University of Technology and University of Gothenburg

Abstract

To reduce the amount of water that is used every day we must be able to efficiently reuse it. Thus, it becomes important to determine if the water is clean enough for reuse. A part of determining the cleanliness of the water is by measuring its ability to conduct electricity. In this thesis a number of different conductivity probes are presented. A low-cost method for measuring conductivity of greywater was evaluated and implemented. The system is based around an ARM microcontroller and uses a probe that can be manufactured in the same way as a printed circuit board which means that this system can be mass produced at a low cost.

Keywords: Conductivity, Greywater, Conductivity Measurement, Embedded, ARM, PCB.

Acknowledgements

I would like to thank my Supervisors Roger Johansson at Chalmers University of Technology, Nicolas Maxant at Mimbly and my examiner Per Larsson-Edefors at Chalmers University of Technology for making this thesis possible. I would also like to thank all my friends and family for their help and support.

Jakob Nolkrantz, Gothenburg, December 2018

Contents

1

Introduction

Sustainable development is becoming more important with time. Clean water in particular is a precious resource in several parts of the world. Therefore, it is important to be able to make products that use less water and are capable of using the same water more than once. To be able to reuse water there has to be a way to determine if the water is clean enough to reuse. A part in determining this is to measure the conductivity of the water. Conductivity can give a reasonable understanding of how many particles there are in the water and in that way give an indication of how dirty the water is. This thesis mainly focuses on developing a low-cost method to measure conductivity. The measurement of conductivity is well established but there is always a need for finding inexpensive and reliable ways of implementation.

The company Mimbly [1] is developing an add-on retrofit system that recycles the water generated by washing machines. The current implementation is rather expensive and could be made at a lower price. In line with the focus of this Master thesis the goal is to reduce the cost of the conductivity measurement system, by introducing an alternative solution to the one that is currently being used. In Mimbly's case the measurement of conductivity has to be able to handle varying degrees of temperature, being able to work for many years and still deliver reliable measurements. This thesis presents the design, verification and implementation of a prototype that can provide an alternative to the current system.

1.1 Problem Setup

The company Mimbly has a system which consists of a water tank that is connected to a washing machine. The washing machine empties its water into the water-tank in between washes. In the tank the water is analyzed during certain stages of the washing process and this determines if the water is clean enough to be reused. A large part of this analyzing process is to measure the conductivity of the water. The equipment currently in use has an on board ARM STM32F303RCT7 [2] microcontroller and it controls several probes and relays that are placed in various parts of the tank.

1.2 Goals and Challenges

The goal is to design an alternative implementation of the conductivity measurement system that Mimbly is currently using. The new design would use the built-in ARM microcontroller instead of the external conductivity chip that is currently in use. The aim is to lower the production cost of the current product by lowering the cost of the conductivity measurement system.

There are several challenges that need to be handled; one challenge is to create a software library that can be used with a standard STM32 Cortex ARM processor. Another one is that the implementation should be able to compensate for temperature variations and have the capability of measuring the conductivity of greywater after given specifications, which implies being able to measure with a precision of 10-100 μS/cm in the measuring range between 100-2000 μS/cm. A third challenge is to test the design with reference solutions and to be able to determine the performance of the new design. The final goal of the thesis is to implement a working prototype on the printed circuit board that could be used by Mimbly.

Presently the probe that Mimbly is using is rather expensive and is also too big to properly fit into the current design of the tank. Therefore, a less expensive replacement would be needed. The replacement probe can either be a purchased probe or a probe specifically designed for the given problem.

2

Basic Theory

The following chapter will give basic theory to the field at hand. The chapter begins with explaining the nature of conductivity in section 2.1. Which is followed by going through some common types of probes in Section 2.2. In Section 2.2.3 the basics of Electrochemical Impedance spectroscopy (EIS) is explained. Different ways to estimate probes impedance curves are explained in Section 2.2.4.

2.1 Conductivity

In 1871 Friedrich Kohlrausch showed that liquid solutions have internal resistance and that diluting a solution increases the resistance of the solution [3]. This discovery showed that solutions have a resistivity which is usually denoted ϱ and is the resistance per centimeter Ωcm [4].

Resistivity, which is caused by the lack of ions to carry electrons in the solution, can be measured to get the conductivity of a solution; the conductivity is the inverse of resistivity and therefore is the ability for a solution to conduct electric current. It has the unit Ω/cm and has the SI symbol σ. When measuring ionic liquids, the conductivity can vary from between 5 μS/m for deionized water and up to several 1000 μS/m for some acidic solutions. Distilled water for instance can have really low conductivity because of the lack of ions while acid solution's such as Hydrochloric acid (HCL) contain more ions and therefore have higher conductivity. Ionic acid HCL and deionized water are used as standard reference solution's for calibrating conductivity measurements, as both have well known values.

Conductivity measurements can be affected by temperature variations which can either have a linear or exponential dependence. For aquatic based solution's the conductivity has a linear relation with the temperature [5].

The variation can be compensated for by using equation $G(ref) = K(t)\big[G(t) - GP(t)] + Gp(ref)$. Here $G(ref)$ is the reference temperature which usually is around 25°C and $G(t)$ is the temperature that is being measured. The variable $Gp(t)$ is the theoretical value of the conductivity at the measured temperature and $G(ref)$ is the conductivity at reference temperature. $K(t)$ is the compensation variable for the difference between theory and reality [6].

2.2 Different Types of Probes

Probes for measuring conductivity can be divided into two categories. Contact probes and noncontact-based probes. Contact-based probes measure resistance while noncontact-based probes measure impedance of the solution. Some types of probes like side plate and parallel probes can be divided into both categories. These probes can either have metal directly against the solution or be covered in some form of isolating coating.

2.2.1 Contact Probes

Contact probes are probes that measure the resistivity of a solution. This method works because ionic solution's conductivity follows Ohm's law closely. These probes can be made of a range of materials. The more expensive ones are made of glass and have contacts that are made of/or covered by platinum or gold. A less expensive type of the probe is printed circuit board (PCB) with copper plates and plated in Electroless Nickel Immersion Gold (ENIG) to protect the copper layer from the environment.

Contact-based probes are usually either two or four poles, the two different types can be seen in figure 2.1 and figure 2.2. Two pole probe works simply by applying an AC or DC voltage and that current will travel between the probe plates. The voltage drops over a known resistor is measured and the change in voltage depends on the resistivity of the solution that is being measured. From the estimated resistance the resistivity can be derived by using the known dimensional properties of the probe known as the cell constant or K value. The K value is usually in the dimension cm^{-1} and has the value of 1. By knowing the probe's K value the resistivity can be calculated from equation $R = \rho * K$ or for conductivity $K/R = \sigma * K$ [7].

Two pole probes have some disadvantages as they suffer from measuring errors caused by added resistance from the measuring cables. In addition, they suffer from polarization which is caused by chemical reaction between the solution and the probes surface when a voltage is applied. If the voltage is a DC signal then probes are going to become polarized where one is plus, and one is minus. This will cause ions of different charges to attach to the poles and the probe will stop working after some time. To prevent this AC voltage is used because of the change in the signal's polarity will protect the poles from becoming polarized.

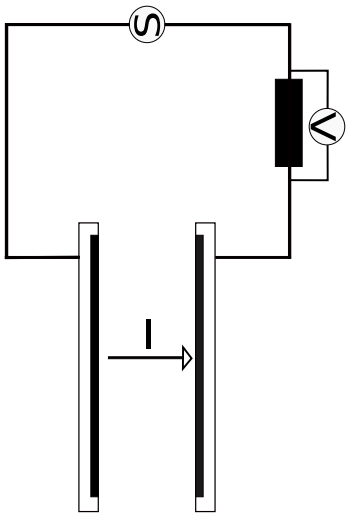

Figure 2.1: Simple schematic of a two pole probe

Probes that use four-poles can be seen in figure 2.1 and figure 2.2, the difference is that four poles probes consist of one inner and out outer plates or rings. The voltage is applied to the outer plate and the potential is measured at the inner. This arrangement enables the use of low current which mitigates polarization. A further benefit of using the four-probe technique is that the added resistance from the cables can be neglected as they cancel each other out.

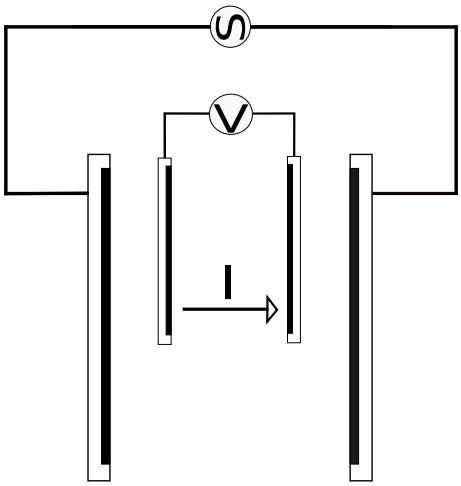

Figure 2.2: Simple schematic of a four pole probe.

Side Plates

Side plates are a version of two pole probes but instead of the plates or cylinders facing each other they are arranged side by side on one surface, as can be seen in figure 2.3. By reducing the probes to one surface the probes can be made smaller, but it also makes it harder to measure the solution's resistance and calculating the K value for the probe. In contrast to parallel plates, these probes use the fringe field effect that is created when a voltage is applied to two metal plates that share

a common border.

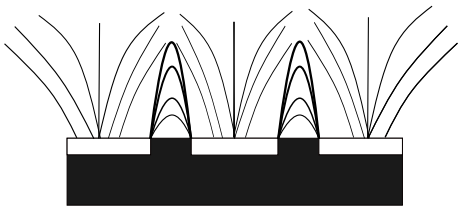

Figure 2.3: The electric field is formed between the parallel plates depicted in white. The bending of the field is known as the fringe field effect

Planar Electrodes

Planar electrodes work in a similar way to parallel plate electrodes and use the fringe field effect. As can be seen in figure 2.4 the probe consists of two parallel plates with a number of fingers extruding from each side where one side's fingers are parallel to the other sides.

There are several studies that use these types of probes, for example a study from 2016 titled "Measuring Electrolyte impedance and Noise Simultaneously by Triangular Waveform Voltage and Principal Component Analysis" [8], uses planar electrodes printed on PCBs as probes.

Because of the shape of planar electrodes, the K value is harder to calculate than for parallel plates. In the study "Theoretical and experimental determination of cell constants of planar-interdigitated electrolyte conductivity sensors" they go through how to calculate the K values and capacitance as well as conductivity of the probes [9].

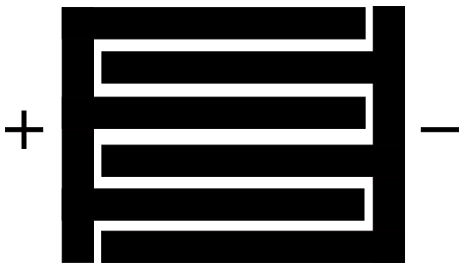

Figure 2.4: The probe consists of N parallel fingers and works in a similar way to side plated probes

2.2.2 Non-Contact Based Probes

The non-contact based probe is either a probe that uses a variation in capacitance or induction. Capacitance based probes use the change in capacitance that occurs when the dielectric medium of the material being measured varies. A probe that use this method is the capacitive plate probe as can be seen in section 2.2.2.2. Inductive probes on the other hand use the variation in magnetic flux caused by the change

of the material in between the two coils. A probe that uses induction is the toroidal conductivity sensor that can be seen in section 2.2.2.1

These types of probes usually consist of metal that is shielded using some type of isolating material. This material can for instance be epoxy coating on top of copper or plastic shielding around inducting coils. This type of protection might be needed in a situation when the metal of the probe might react with the measured solution.

2.2.2.1 Coil Based probes

Toroidal conductivity sensors are sensors that measure the change in inductance. A simplified figure of a conductivity sensor can be seen in figure 2.5. As can be seen from the figure a varying voltage is applied to coil N1 which results in a magnetic field. Over the secondary coil N2 a current is measured that is directly dependent on the change of the magnetic field caused by Coil N1. This magnetic filed depends on the applied voltage and the change of the conductivity in the solution [10] [11].

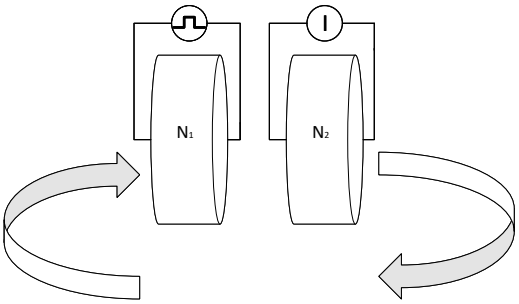

Figure 2.5: Schematic of a toroidal conductivity sensor. A voltage pulse is applied to coil N1 which causes a current to flow in coil N2

2.2.2.2 Capacitive Plate Probes

Capacitive plates are parallel, side and planar plate probes that are shielded from the measured solution. The plate probes are usually covered in some type of resin a common material is epoxy. The resin protects the metal from corrosion but, causes an extra serial capacitance and resistance which makes it impossible to perform measurements using DC voltage. As only alternating current can pass through the capacitive layer. If the protective coating is sufficient, these types of probes don't suffer from polarization like unprotected two pole probes. The capacitance created by the protected layer depends on the thickness and on the permittivity of the coating. Different dielectric material have different effects on the capacitance. The higher the dielectric, the higher the electric field will be, the larger the capacitance. This means that when measuring water compared to air the water will make the probe act as a larger capacitor.

A low cost version of this type of probe is made and tested in the study " A Capacities Fringing Field Sensor Design for Moisture Measurement Based on Printed Circuit Board Technology" [12]. The researchers use a PCB design that is a standard flame retardant grade 4 (FR4) board to measure Capacitance of liquids, the board consists of the FR4 and copper lines covered in resin, meaning that the traces are protected from each other and the environment. The resin is standard FR4 coated epoxy. The researchers utilize the fringe field effect to measure the capacitance of water using a probe looking similar to the structure depicted in figure 2.4. The capacitance is formed between the teeth of the mesh is directly affected by the change of the dielectric of the water.

2.2.3 Electrochemical Impedance Spectroscopy

When a probe is used to measure a solution, the probe can be modeled as a complex impedance equation. To measure this impedance different methods are used. Electrochemical impedance spectroscopy is a commonly used method to derive the impedance characteristic of a system. EIS is an umbrella term for different methods to measure impedance. The basic concept of the method is to apply a known signal and measure the resulting response of the system. Usually this signal is a small voltage amplitude sinusoidal at a fixed frequency measured in a region where the systems response can be assumed to be linear [13].

Measurement with Electrochemical Impedance Spectroscopy (EIS) can be done with different types of stimuli signals ranging from the common sine wave to white noise. The most common one is also the simplest method: The impedance is measured by applying a sinusoidal signal, as can be seen in figure 2.6, with the voltage V as in equation 2.1, at a fixed frequency. The resulting current I as in equation 2.2 and the resulting phase difference θ can then be derived from equation 2.5. By knowing the difference in amplitude between the input and output signals and the phase difference between the signals, the impedance can then be derived from equation 2.3.

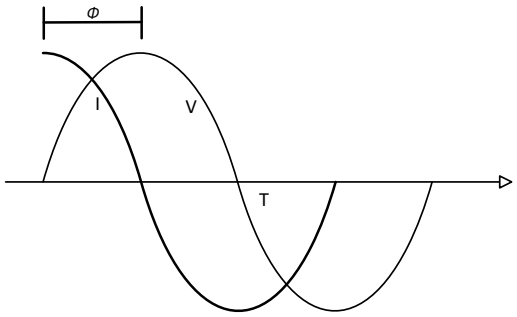

Figure 2.6: Two sine waves where the voltage leads the current

$$V = |V|\, e^{j}(wt + \phi V) \tag{2.1}$$

$$I = |I|\, e^{j}(wt + \phi I) \tag{2.2}$$

$$Z = \frac{V}{I} = \frac{V}{I} e^{j}(\phi V - \phi I) \tag{2.3}$$

$$|Z| = \frac{|V|}{|I|} \tag{2.4}$$

$$\phi V = \phi I + \theta \tag{2.5}$$

An alternative to a sinusoidal signal can be to use transient measurement, where a voltage step signal is used as stimuli and the measured system's response is a time-varying current [14]. Another alternative stimulus is to use Gaussian white noise as input signal can be added to a carrier signal. The resulting value can be measured in the same manner as a sinusoidal signal. There are two types of Gaussian white noise methods: One that uses pseudo random and one that uses (more) random signal [14]. There are stimuli signals that instead of using sine waves, use square waves that are sequenced pseudo randomly and are binary. An example of this type of signal is presented in figure 2.7 [15].

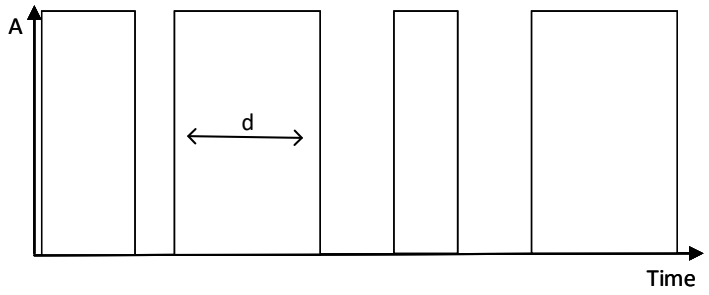

Figure 2.7: A pseudo random square wave signal is a signal which alters pseudo randomly between the low and high state.

When evaluating spectral properties of AC signals Fast Fourier Transforms (FFTs) are often used. The equation for the FFT can be seen in equation 2.6. FFT which is a form of the Discrete Fourier Transform and is used to transform a time-based signal into the frequency domain. This is useful when there is a need to measure the amplitude of a signal at a specific frequency.

$$X_k = \sum_{n=0}^{N-1} X_n e^{-\imath 2\pi kn/N} \; k = 0, 1..., N-1 \tag{2.6}$$

2.2.4 Equivalent Circuits

To be able to transform the measured data to conductivity the measured data is compared to known standard models.The model to be used depends on several different factors: Factors like the size of the probe that is being used, what type of solution that will be measured and the frequency as well as voltage applied to the solution. There are a range of different circuits. The simplest one is the ideal probe where there is no reaction with the measured solution; these probes are referred to as polarizable electrode or blocking electrode. These probes can be seen as a resistance in series with a capacitor [16], where the resistance is the resistance created by the probe's connection to the solution and the capacitance is the effect of the solution's

potential difference to the probe surface.

When representing the impedance measurements of equivalent circuits, usually either Bode plot or Nyquist plot is used. Nyquist plot, which is also known as Cole-Cole diagram is often used in models like the Randles circuit (explained in the section below). When using this method it is possible to determine the value of different parts of the circuit from different points on the curve [17]. A Nyquist plot of the Randles circuit can be seen in the plot in figure 2.8. It can be seen from figure that depending on the frequency used, different components of the Randles circuit can be extracted from the curve.

Least Square Estimation Method

The Least Square Estimation Method (LSEM) is a mathematical method that can be used for estimating how well a measured curve of a system fits with the estimated curve of the same system.

This method is useful to get an understanding on how your system behaves and how much it diverges from the estimated model. When the difference between the measured value and the estimated value is known, changes to the model can then be made to get a better fit between reality and model. Using LSEM and other similar curve approximation methods it is possible to move away from a physical representation of the system. Instead of trying to find an equation that is based in physical explanations of the system, the equation is based on the best fit of the measured impedance. There are downsides to this method as it removes any explanation of phenomena and is only as good as the measured data it is based on.

Randles Circuit

A commonly used equivalent circuit is the John Edward Brough Randles model (Randles Circuit) depicted in figure 2.8. It tries to take into account both kinetic and charge transfer effects. These effects are complex and can be hard to simulate [18].

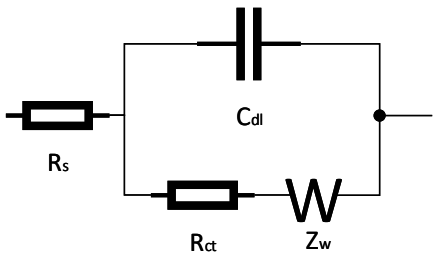

Figure 2.8: Schematic of the Randles Circuit.

The equation for the total impedance of the Randles Circuit can be seen in equation 2.7. From this equation the real impedance can be derived from equation 2.8 and

the imaginary impedance using equation 2.9.

$$Z_w = R_s + \frac{R_{ct}}{1 + w^2 R_{ct}^2 C_{dl}^2} - \frac{jwR_{ct}^2 C_{dl}^2}{1 + w^2 R_{ct}^2 C_{dl}^2} \tag{2.7}$$

$$Z'_w = R_s + \frac{R_{ct}}{1 + w^2 R_{ct}^2 C_{dl}^2} \tag{2.8}$$

$$Z''_w = -\frac{jwR_{ct}^2 C_{dl}^2}{1 + w^2 R_{ct}^2 C_{dl}^2} \tag{2.9}$$

As can be seen in figure 2.8, the Randles Circuit is made up of several components; The capacitance C_{dl} is based on the double layer theory that when a solution containing ions is in contact with another material a double capacitive layer is created. The double layer capacitance can be seen in figure 2.9. The first layer is created by ions affected by surface charge and the parallel capacitive layer which is created by ions affected by the Coulomb force.

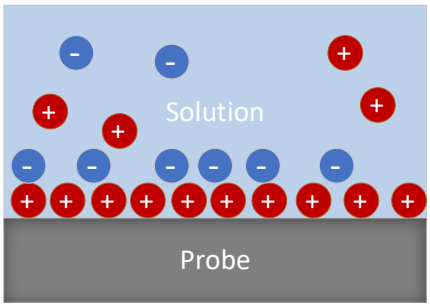

Figure 2.9: Ions in a solution reacting with the surface of the probe

The impedance Z_w is called the Warburg impedance or mass transfer impedance and is the product of ions diffusing in the solution. The diffusion depends on the perturbation frequency. The impedance is high at low frequencies and decreases with the increase in frequency therefore it is usually derived from the Nyquist plot at low frequencies. The Warburg impedance can be described with equation 2.10 where the impedance is equal to the ratio between the Warburg diffusion coefficient σ_w and the square root of the frequency.

The impedance Z_w and R_{ct} are together known as the faradaic impedance Z_f where the real part is R_{ct} and the imaginary part of the impedance is Z_w. The impedance comes from redox (reduction/oxidation) species in solution. The impedance of the solution can vary depending on external heat sources and from the applied voltage from the probe [19].

$$Z_w = \frac{\sigma_w}{\sqrt{jw}} \tag{2.10}$$

The resistance R_{ct} is the charge transfer resistance and R_s is the solution's resistance or uncompensated solution resistance. The solution's resistance is explained

in section 2.2.1. The resistance R_s can be calculated at higher frequencies than Z_w and is at the end of the Nyquist plot, where the plot line intercepts with the x-axis.

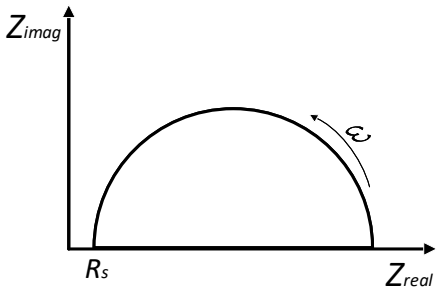

Figure 2.10: As can be seen from the Nyquist curve of the Randles circuit an increase in frequency causes the impedance to go towards R_s

During the years since Randle invented the Randles circuit, several modified versions of the circuit have been suggested. One of these modified versions is presented in the study "Identifiability of Generalized Randles Circuit Models" [20], the authors proposed a general alternative layout. They also proposed ways to identify the different unknown variables by the given input/output response. A figure showing a similar setup as discussed in the study can be seen in figure 2.11.

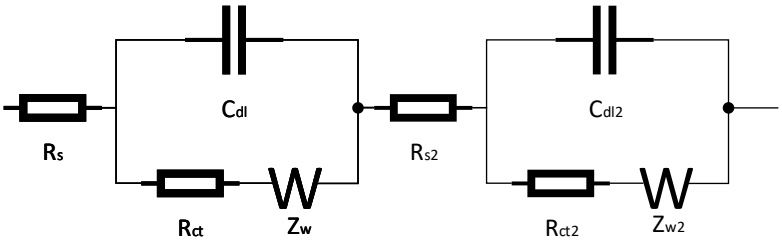

Figure 2.11: Alternative Randles Circuit

Alternative Circuits

A slightly modified representation of an ideal probe can be seen in figure 2.12. Here the equivalent model is based on the one presented in the article " A new probe for measuring electrolytic conductance", In this paper [21] they present a simplified model of a parallel plate probe. In the figure the capacitance C_{ox} is the isolating coating that protects the probe from reacting with the measured solution. The value for the capacitance can be derived from equation

$$C_{ox} = \epsilon\epsilon_r A/d$$

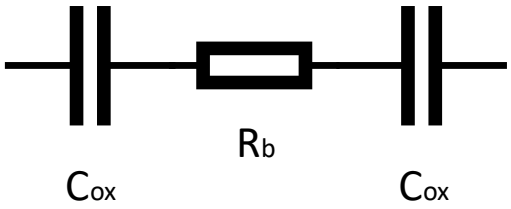

Figure 2.12: An equivalent circuit of a probe immersed in an electrolytic solution

The circuit works on the assumption that by choosing the right frequency a parallel plated probe with an isolating coating has a capacitance that is so large that the other parameters, like the double layer capacity C_{dl} and the faradaic impedance Z_f, can be neglected compared to it.

$$Z_{cell} = \frac{j\omega R_b C_{ox} + 2}{j\omega C_{ox}} = R_b - j\frac{2}{\omega C_{ox}} \tag{2.11}$$

Knowing this and using a input voltage sinusoidal signal the system transfer function would be equal to:

$$\left|\frac{V_{out}}{V_{in}}\right| = \frac{wRC_{ox}}{\sqrt{(wR_bC_{ox})^2 + 4}} \tag{2.12}$$

Using the equation for capacitance given in the study "Capacitive Fringing Field Sensor Design for Moisture Measurement Based on Printed Circuit Board Technology" [12] the capacitance can be calculated from equation:

$$C = \frac{(n-1)\epsilon\alpha\gamma}{d} \tag{2.13}$$

This equation does not take into account the double layer effect as it assumes that any capacitance that is not caused by the isolating layer is so small that it does not need to be taken into account. If this assumption is correct then equation 2.13 can be used.

3

Implementation

This chapter aims to briefly explain the implementation of the system. The chapter begins with a brief overview of the current system under section 3.1. This section is followed by section 3.2 where an overview over the test board is presented. The test board works as a placeholder for the current board that Mimbly is using. To easily be able to test different reference resistors and to protect the built-in op-amp while performing tests a breakout board was designed and implemented in section 3.5. In section 3.4 the design and implementation of an alternative probe is presented. The last section 3.6 explains and shows how the system was tested.

3.1 Current Setup Overview

The current probe that Mimbly is using is a commercially available conductivity probe which can be seen in figure 3.1. The probe can measure in the range between 0.07 μS/cm to 500000 μS/cm. According to the specification the probe has the dimensions 0.012x0.15m [22] [23]. The cost for the probe at the current date 2018-01-21 is around $60.00 US dollars for one unit and $16.00 when purchasing above 5,000 units. The probe is used together with the Atlas scientific conductivity OEM^{TM} circuit which can measure a rage between 5 - 200000 μS/cm and has a resolution up to two decimal places in the range of measurement [24]. The price for the chip as of 2018 ranges from $139.00 for one unit to $124.74 when buying over 25 units.

Figure 3.1: The Atlas Scientific Conductivity probe

3.2 Test Setup Overview

An overview of the test system can be seen in figure 3.2. The system consists of three major parts: The MCU STM32F303, the probe and the breakout board.

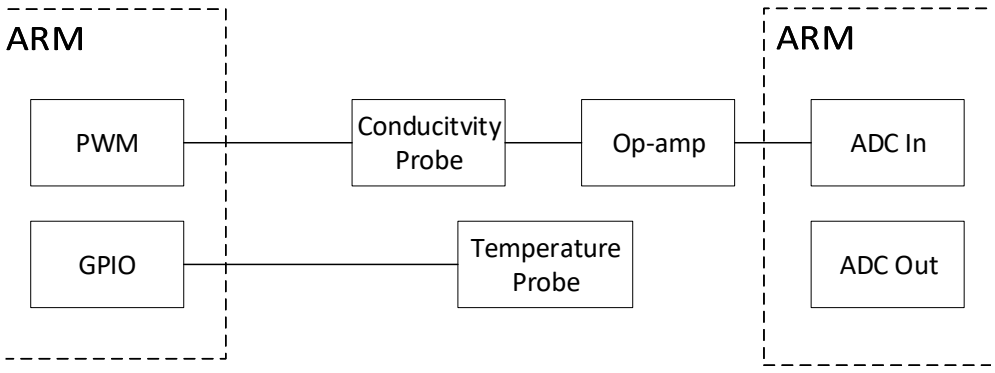

Figure 3.2: An overview of the system, with the same ARM on both side of the figure

3.3 Test Board

Due to limitations in availability of the Mimbly system, a test board was designed to work as a substitute to the board that Mimbly currently is using. On the board is the STM32F303 ARM Microcontroller Unit (MCU), connections for voltage sources, programming input pins for the ARM MCU and output pins for controlling the breakout board. The board also has connectors for the temperature sensor DS18B20 which is mentioned in section 3.3.1, the temperature probe uses a 1-Wire interface protocol to communicate with the ARM MCU. The board was first designed to be used with one Analog-to-Digital Converter (ADC) channel and it was later modified to gain access to two channels. The modification was made so that the input and output signal from the ARM MCU could be measured at the same time. The ADCs on the STM32F303 are covered in section 3.3.2.

The test board can be seen in the result chapter 4.1. The components on the board are listed in table A.1 in appendix, and the pin setup for the board can be seen in appendix A.2.

The initial idea was to use one of the op-amps that are built into the MCU, however op-amps can be sensitive, and it was deemed better to test with an external op-amp first. The internal op-amp is presented in section 3.3.3 where the specifications of the internal op-amp, the possible configuration and usability are shown. The external op-amp is discussed with the breakout-board in section 3.5.

At first the idea was to use a Digital-to-analog converter (DAC), however the problem with using the built in DAC is that it does not have the capability to generate a signal with high enough frequency. As higher frequencies were needed than the DAC could generate, as discussed in section 3.4 a timer was used instead for the DAC. The timer uses the same pin as the DAC so no physical modifications to the test board was needed. The built-in timers of the MCU are covered in section 3.3.4.

3.3.1 Temperature Probe

The Mimbly system uses the temperature probe DS18B20 [25]. The probe can measure with an accuracy of ± 0.5°C in the range of -10°C to +85°C. The maximum possible temperature the probe is capable of measuring is up to 125°C which is well above the maximum temperature that water in a washing machine can reach. The DS18B20 temperature probe uses the one wire communication protocol that has a 64-bit unique code which each unit has and the one wire protocol makes it possible to daisy chain several units.

3.3.2 Analog-Digital-Converter

The ADCs on the MCU are of the Successive Approximation Register (SAR) type. The resolution of the ADCs can be set to either 8,10 or 12 bits. The maximum voltage input of the ADC is 3.3 V, the maximum current the ADC can sink is 20 mA and the highest sampling frequency possible if one ADC is used in standalone mode is 5.39Ms/s.

If the reference voltage $V_{ref} = 3.3\,\text{V}$, the ADC is ideal, and the environment is noise free using 12 bit resolution would then make it possible to measure 2^{12} voltage steps that range between 0 to 4,095. The smallest possible voltage step would then be $\frac{3.3}{4096} = 0.81\,\text{mV}$. Sampling an input signal V_{in} the resulting voltage signal would be calculated from equation $\frac{3.3*V_{in}}{4096}$. This is also known as the accuracy of the ADC and the smallest number is known as the Least Significant Bit (LSB).

The sampling time of the STM32F303xC ADCs T_{SAR} depends on the time between the first and last sample plus the configuration time for start and storing of samples. How fast these samples are sampled depends on the maximum clock frequency of the ARM which ideally should be 72 MHz. The sample rate of the ADC depends on several variables, having the ADC configured for a higher resolution decreases the sampling speed, also the load that is on the ADC has an effect on the sampling speed.

For instance if the resolution of the ADC is set to 12 bit the sampling speed will be less than if it was set to 10 bit as can be seen in equation 3.1.

$$T_{ADC} = T_{SMPL} + T_{SAR} = [1.5_{|min} + 12.5_{|12bit}] * T_{ADC\_CLK} \tag{3.1}$$

Where T_{ADC_CLK} is the clock frequency, T_{SMPL} is the time it takes to sample the signal from beginning to end and T_{SAR} is the successive approximation time which depends on the resolution of the data. From the equation the minimum ADC conversion time for 12 bit resolution would be 0.19μs which is the same as the sampling rate of 5.1 Ms/s.

The STM32F3030xC has four built in ADCs that have access to a total of 16 external channels. The ADCs also have internal connections which makes it possible to measure the reference voltage of the ADCs V_{ref} and has the ability to measure the temperature of the MCU. Not all ADCs has access to all outputs. But all can be set in Multichannel mode which means that the ADC for instance can first sample an input signal from the op-amp and then measure V_{ref}. The ARM has four built in op-amps which are internally connected to the ADCs. This connection makes it possible to use the input of the op-amp and internally send it to one of the ADCs removing the need of having an external op-amp.

ADCs can also be used in dual regular simultaneous mode which makes it possible to sync two ADCs samples. This means that the V_{ref} can be sampled at the same time as an input signal, meaning possibly that some errors caused by the variation of V_{ref} can be compensated. The ADCs are connected two and two to a DMA channel which makes it possible to run the ADCs in parallel with the processor, which reduces the time that measurements take away from other processes that might run on the MCU. The ADCs can also be used in sync, meaning that they can sample the same signal, where one ADC sample on the clock's rising edge and one on the falling edge. This makes it possible to double the maximum sampling frequency [26].

ADCs are not ideal and can differ from what is specified in the datasheet. ADCs can also be affected by the surrounding environment which affects the conversion accuracy, which also can be affected by variations in the voltage reference or because of impedance mismatch between the board and the probe [27]. Some of the error sources can be compensated for in hardware or software.

A common error is the offset error, which is caused when a value which should be either one or zero, instead becomes the opposite value. This is caused by the sampled value being close to 0.5 LSB. This error can be compensated by software after calculating the difference between actual transition minus ideal transition. Similar to the offset error is the gain error; the deviation between an actual reading to an ideal reading. A negative offset exists if the ADC reads the value 4095 before the input signal value is equal to V_{ref} - 0.5 LSB. The gain error is calculated by taking gain error = last actual transition – ideal transition. Both the gain error and the offset error can be compensated for by using the STM32f303 self-calibration mode. This mode will cause the MCU to go into a calibration mode where it uses the ADCs internal connection to the reference voltage as an input signal.

Some errors can be compensated for in software, others by proper hardware config-

uration. One of the errors that can be fixed with either a hardware configuration or software is fluctuation in the reference voltage. One solution is to use one of the built in ADCs to measure the variation in the reference voltage, while another ADC sample the input signal. By simultaneously sample the signals, any variation in the reference voltage would be measured and possibly compensated. An alternative and complementary solution to the same problem is to use a separate power source for the reference voltage. By simply using a separate power supply a potential voltage drop caused by the MCU can be avoided.

In this project the ADC reference voltage source was chosen not to be a separate power source. It was decided after measuring the reference voltage that the signal was stable enough and no drop in the voltage was observed. Also because of the ability to use an ADC to measure the reference voltage at the same time as the input signal is being sampled.

When using a non-ideal power supply and especially switched-mode power supplies, noise is generated. Some steps were taken to minimize noise generated by the power supply. A low-dropout voltage regulator (LDO) was placed after the 5 V power source to down convert the power and also lessen the ripple caused by the switched power supply. A capacitor of the size 100 nF was placed between the ground and the main power supply to filter out high frequency noise.

3.3.3 Internal Operational Amplifier

The STM32f303 chip has four built in op-amps. The built-in op-amps have their outputs internally connected to the inputs of the ADCs. The op-amp has external connections accessible for both outputs, the non-inverting and inverting input pins. This makes it possible to use the op-amps in any configuration. The bandwidth of the op-amps is 8.2 MHz which means that they should be able to handle frequencies that are above the frequencies that the ADC can sample. The op-amp has the ability to do rail-to-rail which is important if the measuring range is up to 3.3 V as otherwise the op-amp would not be able to properly handle the highest voltage level.

3.3.4 Timer

A timer was used to generate a Pulse-width modulation (PWM) signal which is used as the input signal to the system. A timer was chosen as the built in DAC is not capable of handling frequencies around 1 MHz. The maximum current that the timer can source is 20 mA which is enough for the system as the ADC can not sink more.

3.4 Probe

In the following section the probe design is presented, simulations on the probe are performed in section 3.8 and the final results are presented in the result chapter. The probe is based on the theory of capacitive sensor probes and the idea is to use physical models presented in the theory section and modify existing equivalent circuits, like the Randles circuit, to create a model that can be used to describe the behavior of the probe. The design steps of the probe can be seen in the flowchart in figure 3.3. The theory and physical models steps are presented earlier in the theory section. The mathematical model and the equivalent circuit steps can be seen as one step as the circuit is in a way a mathematical representation of the probe. The last steps are the measurements and equation fitting steps. These steps are used to test the probe and if it turns out that the model does not fit the design then the model either has to be changed or modified to fit the probe's behavior.

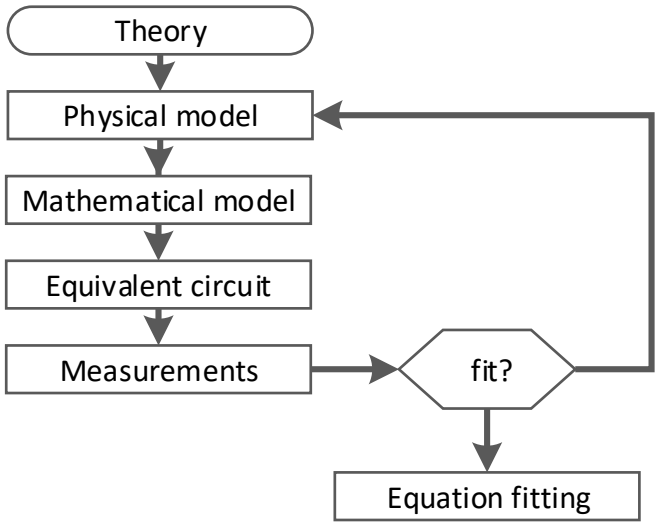

Figure 3.3: Flowchart over probe evaluation.

The type of probe chosen in this thesis was a parallel capacitance probe made out of FR4 board. The probe was chosen due to being inexpensive to produce and no real extra assembly was required except for adding cables to the probe. This means that the manufacturing cost of the probes can be kept low. The design cost is minimal as the probe can be designed with the free software Kicad which is the same software that is used to design the test and breakout board. Probes ordered from a manufacturer would range from 5 US-dollar for 5 probes down to cents if ordered at higher quantities. The parallel plated type of probe has one major advantage over both side plates and finger plates: when it comes to durability, parallel plated probes will not as easily be short-circuited by detergent that might start to form between the plates as there is empty space between the plates. Both the side and finger plate probes consist of one board which means that detergent can get stuck

on the board and form a connection between the plates.

An estimated equivalent circuit for the parallel probe can be seen in figure 3.4, the equivalent circuit is based on the Randles cell presented in the theory chapter. The dimensions of the probe can be seen in table 3.1, where the length between the probes was set to be equal to 0.1050 m as it is the distance between the walls of the Mimbly tank and according to the manufacturer the thickness of the epoxy should be around 20-30μm [28]. The probe after manufacturing can be seen in figure A.5 in appendix A.

Table 3.1: The probe's dimensions

Plate Area	0.0012 m^2
Epoxy thickness	35μm
Probe width	0.044 m
Probe Height	0.1 m
Distance between probes	0.1050 m

In the equivalent circuit in figure 3.4. the cable's resistance R_{cables} depends on the length of the wires between the probe and the board. The capacitance C_{FR4} is created by the connection between the FR4 plate, the copper plate and a material or liquid interacting with the FR4 board. The probes will be placed against the inner wall of the tank which is made out of plastic, which results in the capacitance C_{FR4} being so small compered to the capacitance C_{epoxy} that it can also be neglected.

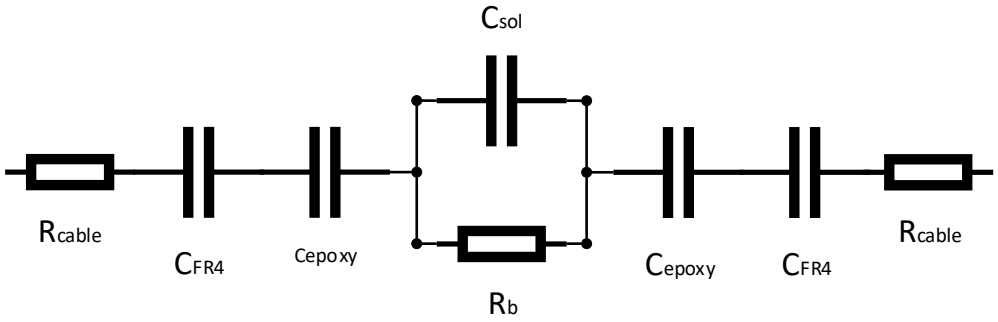

Figure 3.4: Parallel probe in solution equivalent circuit.

The capacitance C_{epoxy} is the largest capacitance of the probe and is created by the copper-epoxy layer interacting with the water. The size of the capacitance can be calculated using equation $C_{epoxy} = \epsilon_0 \, \epsilon_{epoxy} \, A/d$. Using the values presented in table 3.1 where A is the area of the plate and d is the thickness of the epoxy. Assuming that the epoxy is 35μm which is in the middle between the high and low value. The dielectric constant is $\epsilon_0 = 8.8541{*}10^{-12}$ and the epoxy dielectric ϵ_{epoxy} is assumed to be around 4.

The capacitance of the water can be calculated using equation $C_{sol} = \epsilon_{sol}\ \epsilon_0\ A/l$, different from the epoxy capacitance, the solution capacitance changes with the amount of salt and the heat of the water. Washing machine water can have a temperature ranging between 30° to 90°C and causing the dielectric constant of the solution ϵ_{sol} to vary between 58 to 76 [29]. This means that ϵ_{sol} is 18 times larger at 90°C than at 30°C meaning that ϵ_{sol} will have the highest value at 90°C. The capacitance C_{sol} will then have its highest possible value when the washing machine water is at 90°C and is close to being distilled water, meaning that it lacks nearly any salts. The capacitances C_{sol} can be seen in table 3.2 where ϵ_{sol} is assumed to be between 50-80. The capacitance will affect the impedance measurements; however, these values are the worst case and as the conductivity increases, the capacitance will go down, meaning that in theory this value could also be neglected. The resulting values for the capacitance can be seen in table 3.2.

Table 3.2: Approximate size of the capacitance of the equivalent circuit

C_{sol} 80	8.0952 pF
C_{sol} 50	5.0595 pF
C_{epoxy}	1.2143 nF

The solution's resistance R_b can be calculated from the conductance of the solution and the cell constant K. The K constant can be calculated from $K = (l/A)$, where l is the distance between the probes and A is the area of the copper plate on the probe. The cell constant for the parallel probe in this thesis is equal to 0.8571 cm^{-1}, assuming that K actually is a constant. However, this is not exactly true and the value of K might not exactly be equal to the ratio (l/A) as the equation is a simplification. Also the constant K might also vary depending on the heat and the conductance of the water. To compensate for this possible variation, the form factor variable f is introduced to equation $K = (f * l/A)$. The resulting solution resistance R_b, when the conductivity is between 100 - 2000 μS/cm, is calculated for different values of the form factor and can be seen in table 3.3.

Table 3.3: Estimated solution resistance based on different form factors

f	Resistance R_b
0.1	50 −300 Ω
0.25	107 −2143 Ω
0.5	214 −4286 Ω
1	429 −8571 Ω

3.4.1 Simplified Probe

The equivalent circuit in figure 3.4 can be made even simpler assuming that the only capacitances in the system is the epoxy layer C_{epoxy} and the solution C_{sol}. Further simplifications of the model is possible if the frequency of the voltage signal is kept constant at a suitable frequency. Then it should be possible to also neglect C_{sol}, leaving only R_b and C_{epoxy} as in the circuit shown in figure 3.5.

As any other impedance component in serial with C_{epoxy} will produce an offset bias voltage, when measured by the system, such other components can also be neglected. The simplification is only valid if the epoxy capacitance is high enough and there exists no other capacitance in series with the liquid's resistance R_b. If a capacitance does exist and it is in series with the liquid then that would have to be taken into consideration. As mentioned in the theory section, if the epoxy capacitance is large enough the other capacitances can be neglected. Exactly how much larger the epoxy capacitance needs to be is not exactly known, it was assumed that it should be in the area of magnitude of a few nanofarad larger than other possible capacitances [21]. The manufacturing process of the FR4 is not perfect and the variation of the epoxy solder resist layer added on the PCB varies. Therefore it is important to make the size of the plates of the probe large enough to create a large capacitance, but not so large that the system cannot measure it, or make the size of the plates so large that the plates do not fit into the design of the tank.

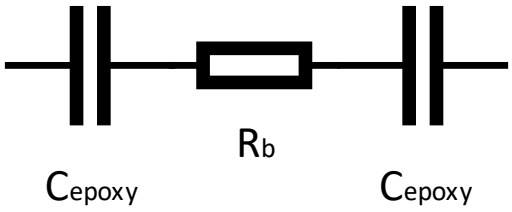

Figure 3.5: The simplified circuit.

3.5 Breakout Board

As mentioned in section 3.3.3, the STM32F303 MCU has four built-in op-amps that have externally accessible pins. To be able to easily test different configurations an external op-amp was configured as an transimpedance amplifier. This op-amp was placed on a separate PCB (breakout board), see figure 3.6. The 5 V pin from the test board is fed from the board directly to the 5 V input pin on the op-amp. Not shown in the figure is a capacitance that is used as a filter for removing interference on the 5 V power line. Also not shown is a voltage divider which is used to give the single supply op-amp an offset voltage. The PCB schematic of the board can be seen in appendix A.1 and the PCB for the breakout board can be seen in figure 4.3 in the result chapter.

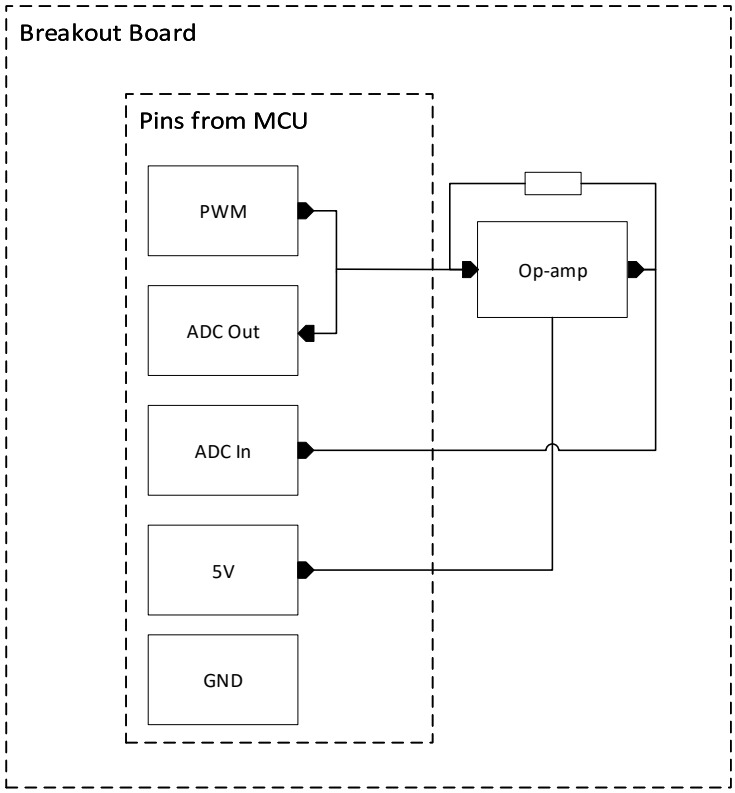

Figure 3.6: Block diagram overview of the Breakout board.

The op-amp on the breakout board works as an active current-to-voltage converter where the resulting voltage from the op-amp is measured by an ADC. By using the op-amp as an current-to-voltage converter the ratio between the input voltage and the output voltage divided by the feedback resistor can be used to derive the impedance of the probe.

The value of the feedback resistor R_f can be calculated from the sinking current limit of the ADC, which is 20 mA as mentioned in section 3.3.2 and according to section 3.3.4 the maximum voltage that the timer can generate is 3.3 V. Knowing the maximum voltage and current the minimum impedance that the system can measure can be calculated to be 165 Ω. The highest impedance the system can measure is limited to the resolution of the ADC and the size of the feedback resistor. If the feedback resistance was set to be 1 Ω and the system was fed with 3.3 V. Knowing that the resolution of the ADC is 0.81 mV, the maximum resistance that the system could measure would be 4071 Ω.

The optimal value for the feedback resistor would be a value close to the lowest impedance value the probe can become. Based on values in table 3.3, it can be assumed that the impedance of the system is above 165 Ω. To be safe R_f was chosen to be 220 Ω. If the resistance of the solution is lower than the feedback resistor, a resistor R_s can be placed in series with the probe. Raising the measured impedance above the resistance of R_f, making it possible to measure a solution's resistances R_b, that is lower than the reference resistance.

3.5.1 Breakout Board Operational Amplifier

The operational amplifier used in the project was the NE5334 [30], chosen because it fitted the required criteria of having a bandwidth above 1 MHz. The idea was that if the measurements worked with an op-amp that has lower specification then the built-in op-amps, then it should also work with the built-in op-amps. Therefore the external operational amplifier was chosen since it should be able to work as an alternative to the built-in op-amp.

The op-amp would also have to work using a single supply as the built-in op-amp is single supplied. The main difference between the on-board op-amp and the one used in the experiments is that the built-in uses 3.3 V while the external uses 5 V. According to the datasheet for the external amplifier, it needs an offset of at least 2 V to be able to function properly with this type of signal. Measurements showed that the operational amplifier worked better at voltages close to 2.5 V. If instead the built in op-amp on the MCU is used, the V_{ref} would be equal to 1.65 V. This means that using the built-in op-amp would allow for a 0.8 V higher voltage swing, which would increase the resolution of the system.

3.6 Program Setup Overview

The system software is outlined in the flowchart shown in figure 3.7. The program starts with an automatic calibration of the ADCs. This is followed by the start of Timer1 which is used to start Timer2. Timer2 generates a PWM signal which is the output signal of the system. Timer1 also starts two ADCs, one that samples the PWM output signal before the probe and one that samples after the op-amp. By starting both ADCs and PWM signal at the same time the system remains synchronized.

By using Direct Memory Access (DMA) together with the ADCs, the values sampled from the ADCs can be stored directly to the memory. The reason for using a timer to start the process and a DMA is to free up time for the processor to execute other operations that might be performed on the MCU. When using one DMA the signals get stored together as one long string, therefore the array needs to be sorted to be able to retrieve the original signals.

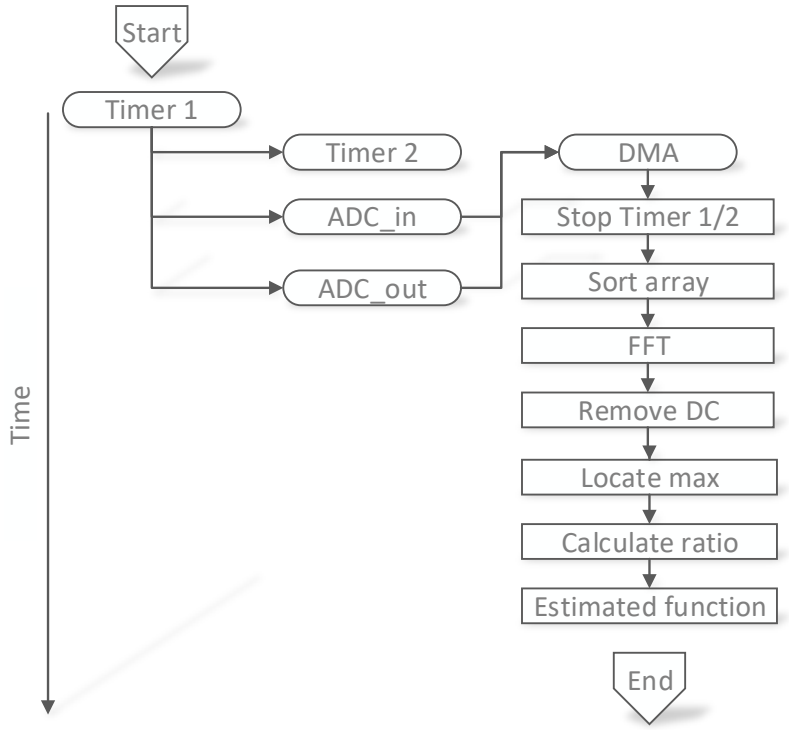

Figure 3.7: Flow diagram covering the program setup.

After the signals have been retrieved a fast Fourier transform (FFT) is used to transform the signals from time into frequency domain and after the FFT the DC part of the signals are removed.

By choosing the fundamental frequency for the calculations the maximum amplitude for the signal can be located. The maximum values of the signals are then divided by each other and the resulting ratio is used in a fitness function. The functions use the ratio and relates it to conductivity. When the calculation is done the sequence starts over or ends.

3.7 Mathematical Estimation of the System

Before performing computer simulations, a mathematical equation was used to estimate the behavior of the system. A system using the simplified probe circuit seen in figure 3.5, can mathematically be represented using equation 3.2.

$$V_{in} = \frac{V_{out}\omega C_{ox} R_f}{\sqrt{((\omega(R_b + R_s)C_{ox})^2 + 4)}} \tag{3.2}$$

The resulting input voltage V_{in}, with added bias voltage to varied value of conductivity $(1/R_b)$, can be seen in figure 3.8. In the figure the output voltage was set constant to 3.3 V, the purple line is 1 MHz and the yellow line is 10 MHz. The component values for the equivalent probe can be seen in table 3.4, assuming that the form factor is 1.

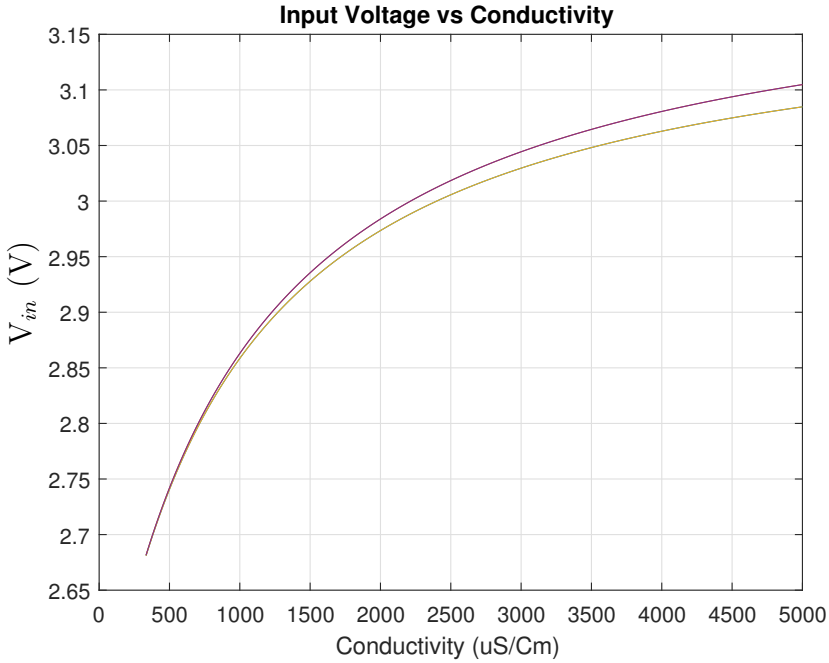

Figure 3.8: The resulting input voltage to varied conductivity.

Equation 3.2 can be rewritten to equation 3.3 to get the solution resistance R_b. Using this equation and the values in table 3.4, it is possible to get an estimation of the expected resistance of the solution to the conductivity.

$$R_s + R_b = \frac{\sqrt{(\frac{V_{out}}{V_{in}})(\omega C_{epoxy} R_f)^2 - 4}}{\omega C_{epoxy}} \tag{3.3}$$

For the highest conductivity the solution resistance R_b is equal to 439 Ω. Using equation 3.2 the estimated resistance of the solution equals 382 Ω, when the frequency is equal to 1 MHz and for 10 MHz the estimated resistance is 443 Ω.

When the solution resistance is set to 8571 Ω the estimated resistance becomes 8585 Ω at 1 MHz and for 10 MHz it becomes 8514.3 Ω. It is clear that the impedance goes towards the resistance as the frequency increases, at least when it is assumed that the capacitance C_{sol} is zero.

Estimated impedance for varied range of conductivity can be seen in the graph in figure 4.7, in the result section. From the figure it can be seen that as the conductivity increases, the impedance goes towards zero. Therefore, to better measure lower resistance a resistor R_s with the value of 1000 Ω was placed in series with the probe to increase the solution resistance R_b above the reference resistance R_f.

Table 3.4: The values used for the calculations

ω	2π*10^6 rad/s & 2π*10^7 rad/s
R_b	439 Ω to 8571 Ω
R_s	1000 Ω
R_f	220 Ω
C_{epoxy}	1.2 nF

3.8 System Simulations

Computer simulations were used to estimate how well the system could measure the resistance of the solution R_b, which frequency the measurement should be done at and what impact the capacitance C_{sol} has on the measurements. The resistance for the solution can be seen in table 3.3, where the form factor $f = 1$. Simulations of the system's hardware was done using Linear Systems Spice Simulator LTSPICE IV [31]. The simulation setup can be seen in figure 3.9. The values for the simulation are taken from tables 3.2 and 3.3 in section 3.4. Simulations using the setup in figure 3.9 can be seen in figure 3.10, figure 3.11 (zoomed in version of 3.10) and in figure 3.12 where $R_b = 8571$ Ω.

3.8.1 Simulation Setup

Starting from the left side of figure 3.9, it shows a timer generating V_{out} a 3.3 V square wave pulse from the ARM MCU. The signal travels through an equivalent circuit of the probe. From the equivalent circuit of the probe the signal goes to the op-amp which is configured in transimpedance configuration. Negative feedback is provided to the system through the resistance R_f from the input to the output pins on the op-amp. The input voltage goes into the inverted input pin of the op-amp and then from the op-amp into the ADC on the ARM.

The impedance of the probe can then be calculated in software by dividing the input voltage with the value of the resistance of the feedback resistor. The value of the feedback resistor depends on the smallest impedance value that will be measured. If the value is too small relative to the feedback resistor the input current will become higher than the maximum current that the ADC can measure. A reference voltage is applied to the positive pin of the op-amp. An offset voltage of 2.5 V is added to the input signal which limits the voltage swing to 0.8 V.

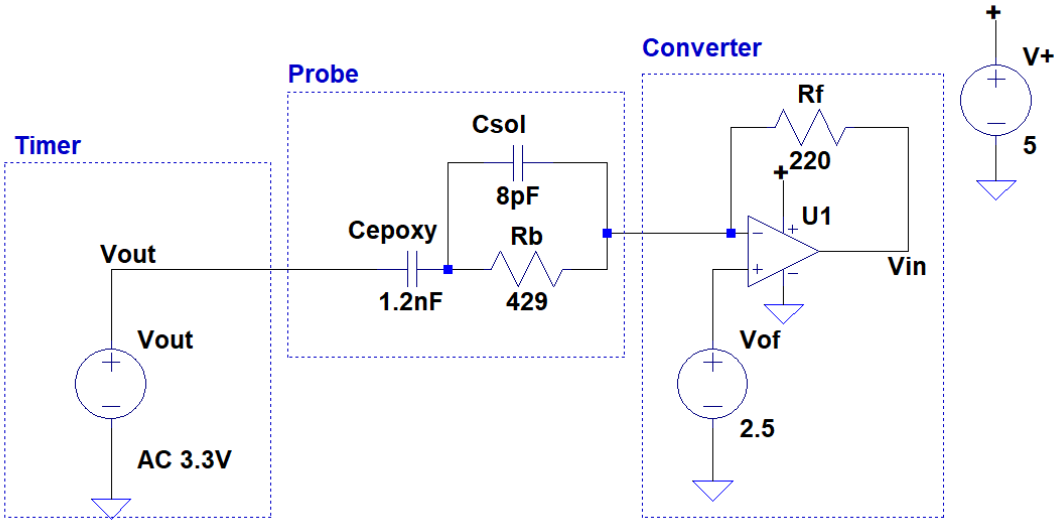

Figure 3.9: The Setup of the simulation for $C_{sol} = 8\,\text{pF}$, $C_{epoxy} = 1\,\text{nF}$, $R_b = 429\,\Omega$.

3.8.2 Frequency-Domain Simulations

In the following simulations the capacitance C_{epoxy} is kept constant at 1.2 nF. The solution resistance R_b is tested using the lowest estimated value for the resistance 429 Ω and 8571 Ω as the highest.

Figure 3.10 shows how the estimated impedance of the probe changes with the frequency. It can be seen that at higher frequencies the total impedance of the probe goes towards the value of the resistance R_b. The simulation was done with C_{sol} being equal to 8 pF as the blue line and 1 pF as the red line in the figure.

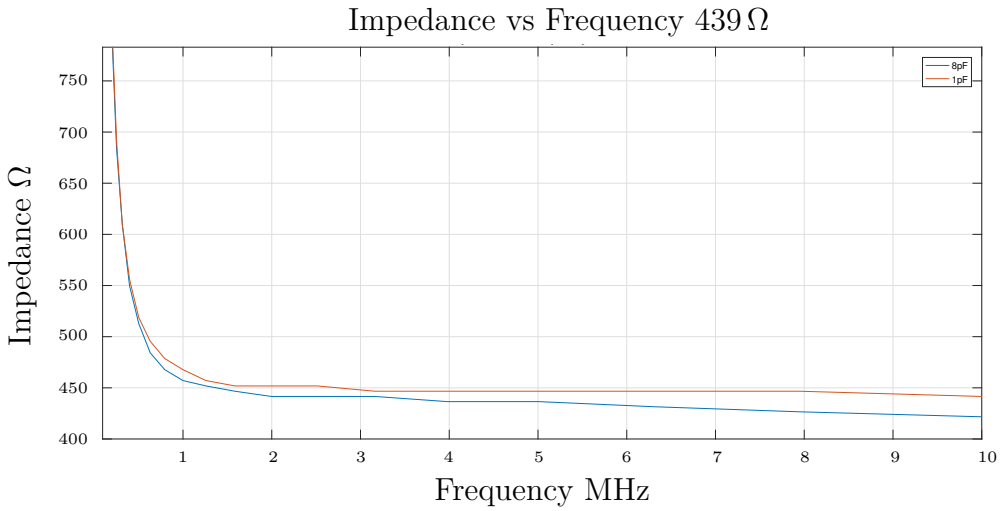

Figure 3.10: $R_b = 429\,\Omega$. The estimated impedance = 458.4Ω at 1 MHz when C_{sol} = 8 pF and is 465Ω when C_{sol} = 1 pF.

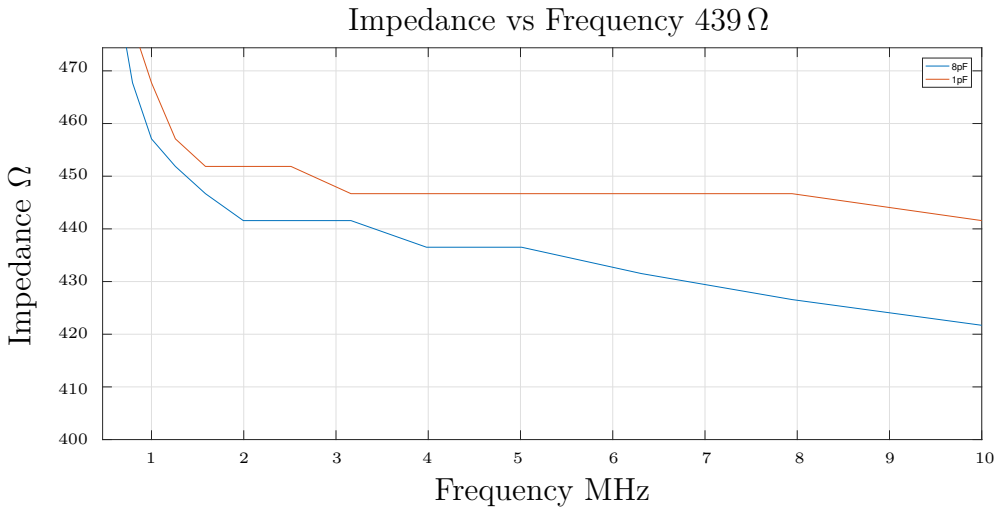

Figure 3.11: Zoomed in version of figure 3.10.

It can be seen in figure 3.12, that capacitance C_{sol} has an effect on the impedance. The difference in impedance between the simulation where the probe has the capacitance C_{sol} = 1 pF and the simulation where it has the value 8 pF, increases with increased frequency.

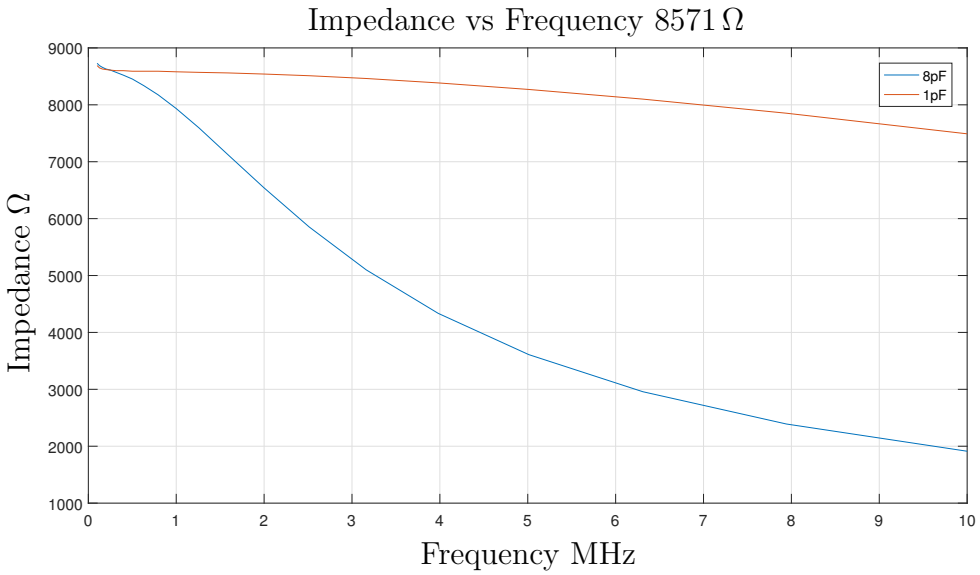

Figure 3.12: Simulation where $f = 1$, $R_b = 8571\Omega$. The resulting impedance = 7923Ω when $C_{sol} = 8\,\text{pF}$ and equals 8580Ω when $C_{sol} = 1\,\text{pF}$

.

3.8.3 Transient Simulations

To get a better understanding of the behavior of the system, transient simulations were performed with a fixed frequency of 1 MHz. The simulations setups are the same as described in section 3.8.1 except that C_{sol} is assumed to be zero, $C_{epoxy} = 1\,\text{nF}$, $R_b = 560\,\Omega$ for figure 3.13 and $R_b = 8200\,\Omega$ for figure 3.14. The values were chosen to be able to perform tests using a breadboard and to use the standard e12 series of component values. As not all values are part of the e12 series there will be a difference between the component values and the actual values. The difference for the capacitance C_{epoxy} is 0.83, for the resistances $560\,\Omega$ it is 0.76 and for $8200\,\Omega$ it is 0.96.

In the figures the red wave is the output voltage $V_{out} = 3.3\,\text{V}$ and the blue is the input voltage V_{in}. The difference in V_{in} between the simulation is 0.8 V, when using resistances $560\,\Omega$ and $8200\,\Omega$. This would mean that the voltage the system will measure over would vary over a voltage range of 0.8 V.

To see how the system would work in practice, tests were made using: The test board, breakout board and an estimated probe realized on a breadboard with the same component values as in the previous simulations. The resulting values from the test can be seen in figures 4.4 and 4.5 in the result chapter. In these figures it can be seen that the measured values have more interference compared to the simulated, but otherwise closely follows the simulated values.

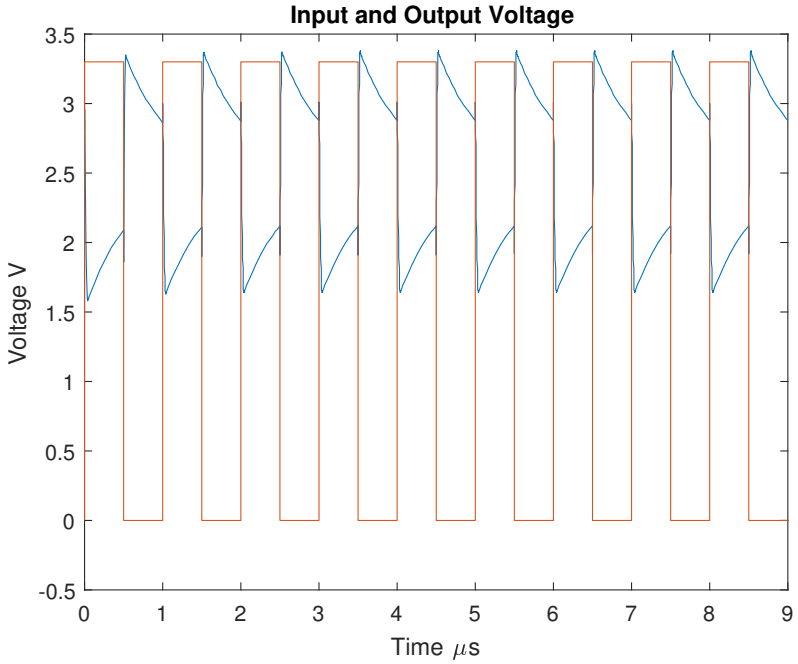

Figure 3.13: $V_{out} = 3.3\,\mathrm{V}$ at $1\,\mathrm{MHz}$, $C_{epoxy} = 1\,\mathrm{nF}$ and $R_b = 560\,\Omega$.

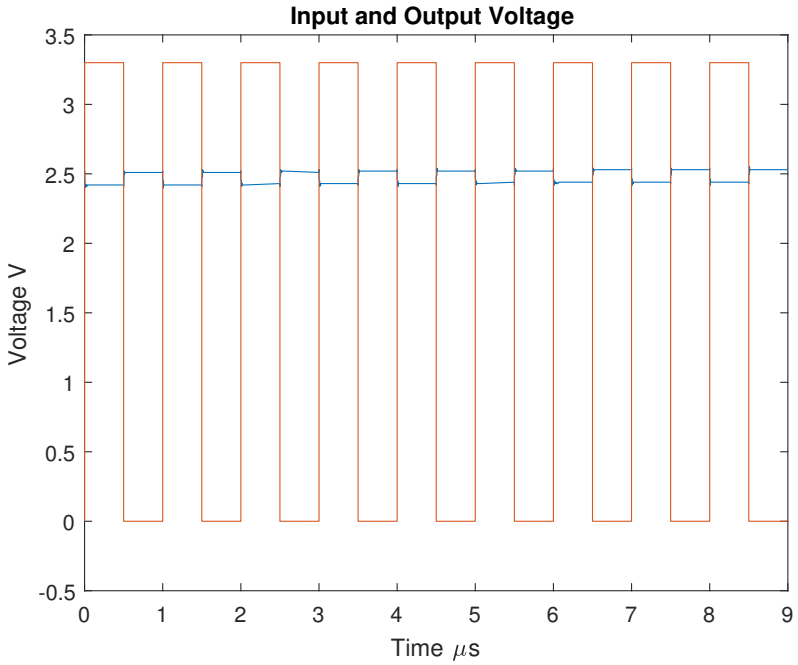

Figure 3.14: Same simulation as in figure 3.13 with $R_b = 8200\ \Omega$.

4

Results

In this chapter the results of the project are presented, starting with the hardware (the hardware components of the test board, the breakout board and the schematics are described in appendix A). Next we will describe system-level measurements using the probe (the test setup can be seen in appendix A).

The test board developed in this project can be seen in figure 4.1. The board uses the ARM STM32F303xC microprocessor and was made with the purpose of being able to supply power and measure the output from the breakout board as well as the input from a temperature probe.

To make it possible to read the input and output of the breakout board at the same time a modification to the PCB was made. This modification adds an additional ADC and can be seen in the figure, as the additional wires connected to the MCU.

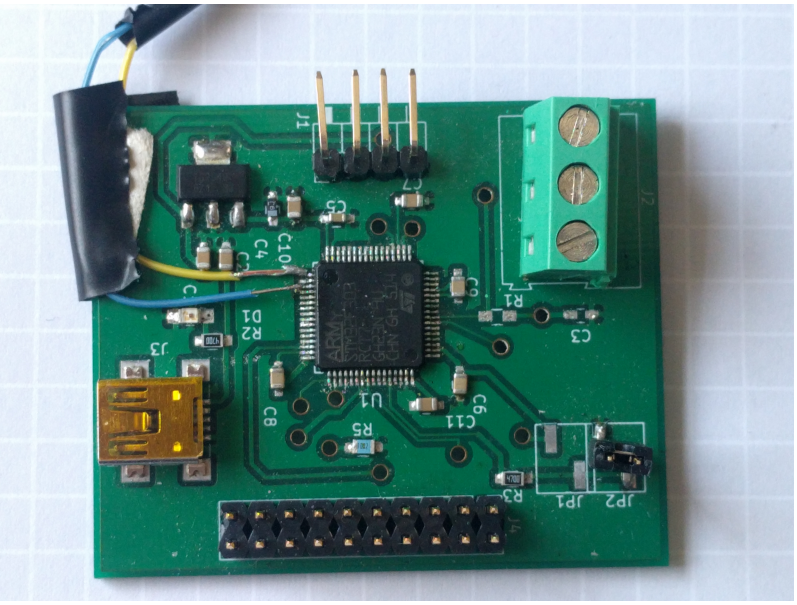

Figure 4.1: The test board with the op-amp in the middle of the PCB.

The breakout board, which can be seen in figure 4.2, the board consists of an op-amp in a transimpedance amplifier configuration.

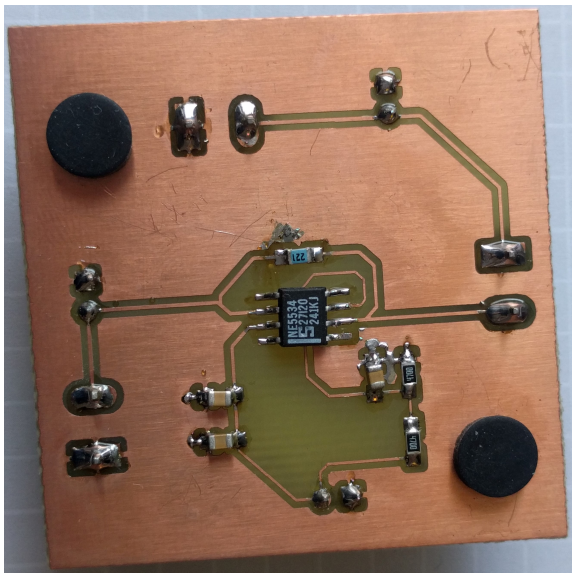

Figure 4.2: The breakout board with the op-amp in the middle.

The resulting parallel plated probe can be seen in figure 4.3. The dimensions of the probe can be seen in table 4.1.

Figure 4.3: The finished parallel plated PCB probe.

Table 4.1: The probe's dimensions

Probe Area	0.0012 m^2
Epoxy thickness	35μm
Total Length	0.044 m
Total Height	0.1 m

4.1 Hardware verification

To verify that the hardware worked as intended, test were performed using the test board and breakout board. The test consisted of connecting the test board to the breakout board and the breakout board to a breadboard. The estimated probe circuit on the breadboard had the values $C_{sol} = 1\,\text{nF}$ and $R_b = 560\ \Omega$.

The results from the test can be seen in figures 4.4 and 4.5. The figures show the input and output signals measured using an oscilloscope. In these figures the yellow wave is the output voltage and the blue wave is the input voltage. The voltage offset can be seen in figure 4.4. By removing the offset, it is easier to see the change in the signal, as can be seen in figure 4.5.

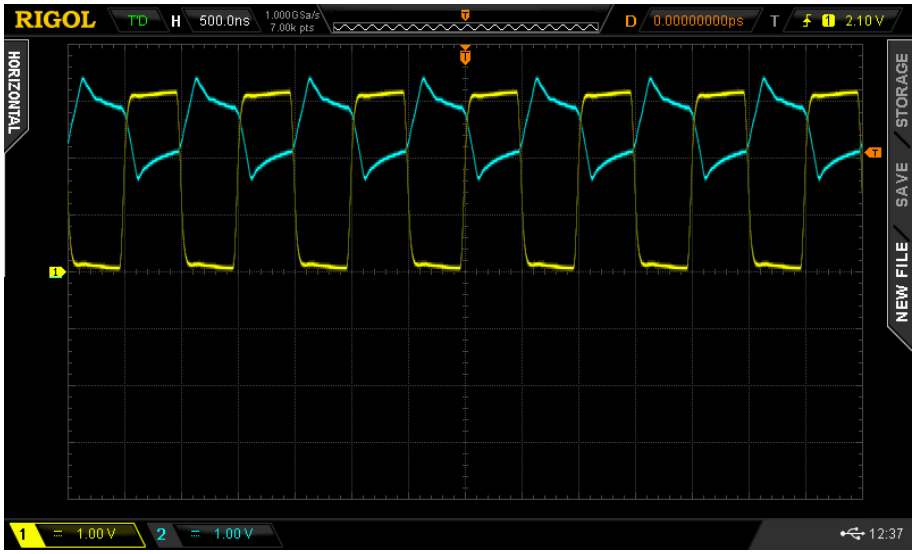

Figure 4.4: Oscilloscope image of the input and output voltage, when a 1 MHz square wave is applied to the system where $C_{sol} = 1\,\text{nF}$ and $R_b = 560\ \Omega$.

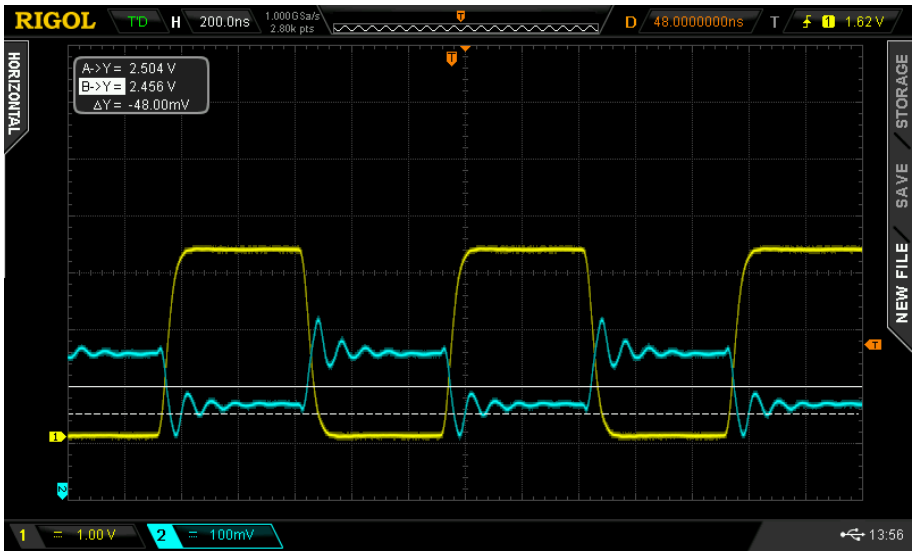

Figure 4.5: Oscilloscope image centred around the DC level of the input and output voltage when a 1 MHz square wave is applied to the system where C_{sol} = 1 nF and R_b = 8200 Ω.

4.2 System verification

The measured impedance relation to the conductivity can be seen in figure 4.6. As a reference probe the conductivity was measured by the Atlas scientific probe [23]. The measured solution consisted of a mixture of tap water at 20°C and washing machine detergent. The probe used to measure the impedance is the probe shown in figure 4.3. The test setup can be seen in appendix section A.3 and the values for the setup used for the measurements can be seen in table 4.2.

Table 4.2: Variables used in the graphs.

ω	2π*10^6 rad/s
R_s	1000 Ω
R_f	220 Ω

The water mixture was sampled at a starting interval of 200μS/cm, increasing the sample interval as the conductivity nears 2000μS/cm. This is needed as smaller changes in impedance have a higher effect on the resulting measured conductivity. The plot can be compared to the simulated plot shown in figure 4.6, which the figure does not depict the uncertainty of the measurements. The resolution of the ADC is 0.81 mV, which would cause problems at higher conductivity. Another factor is the variation in temperature as the water temperature is slow to stabilize and varies between sample points.

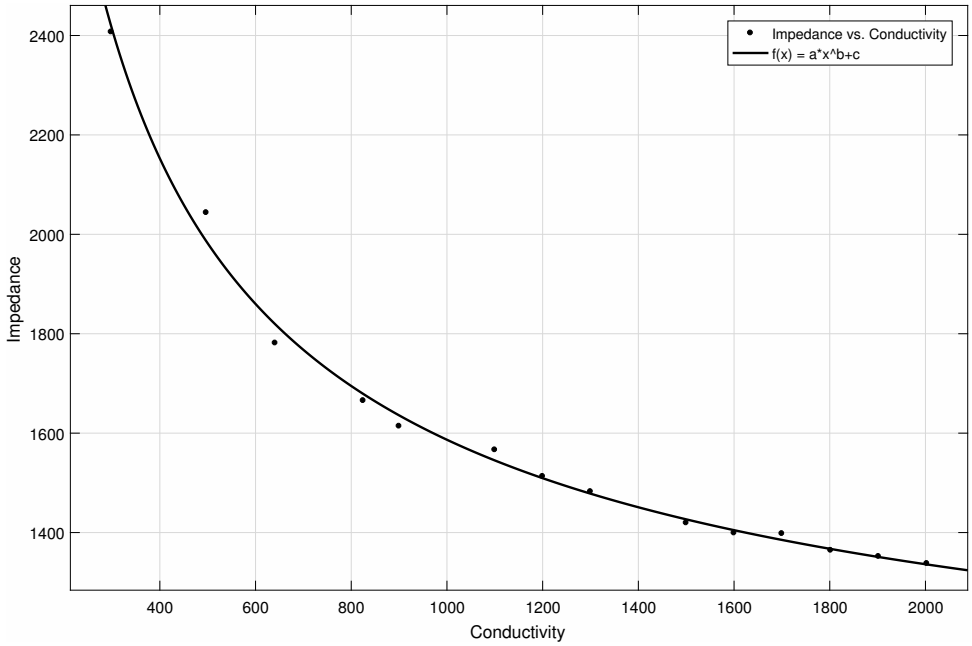

Figure 4.6: Data points matched with exponential equation.

Comparing the result from figure 4.6 with the calculated values in the figure 4.7, in which the blue line is for the 1 MHz frequency and the red line is for the 10 MHz. The input voltage for the curves was derived using equation 3.2 and equation 3.3 was used to calculate the resistance. The conductivity was then calculated from $\frac{1}{R_b}$. The impedance could then simply be extracted from $\frac{V_{in}}{R_f}$, where R_f is equal to 220 Ω.

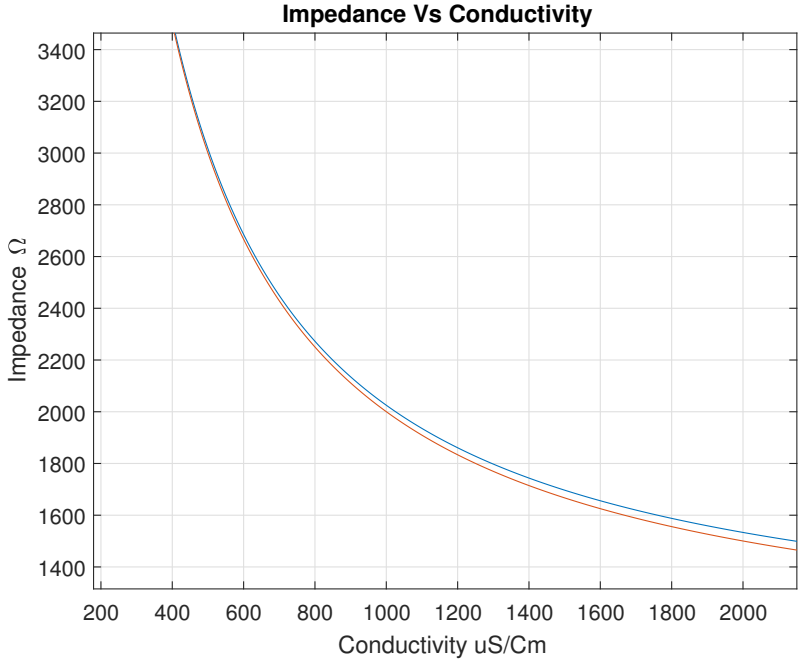

Figure 4.7: Plot showing the relation between the impedance and the conductivity $R_s = 1000\,\Omega$, $R_f = 220\,\Omega$.

Figure 4.8 shows a comparison between the blue line in figure 4.7 and the measured values. The red-line is the estimated curve from the measured values in figure 4.6 and the blue-line is the estimated values from figure 4.7.

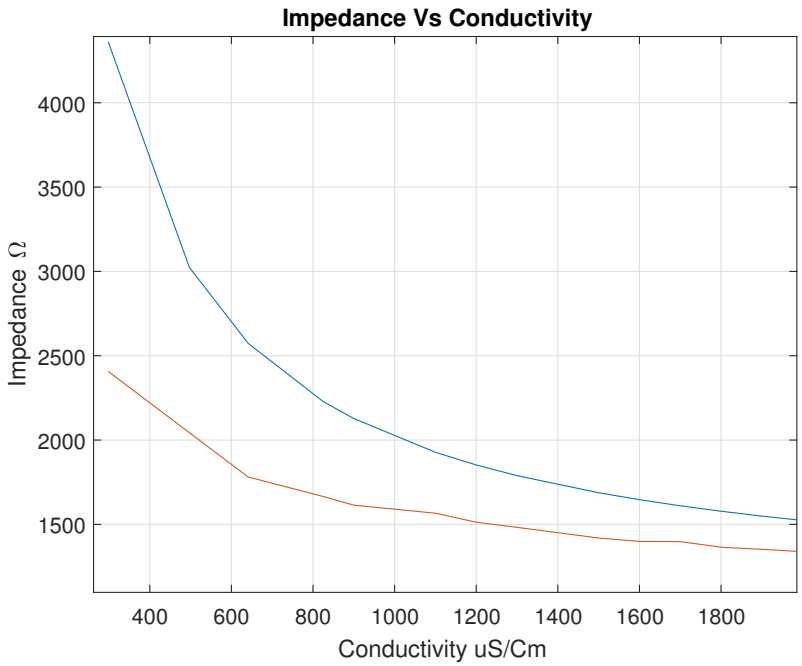

Figure 4.8: Plot showing the relation between the impedance and the conductivity R_s 1000 Ω, R_f 220 Ω.

A simplification of the measuring method presented in figure 4.7 can be seen in figure 4.9, where instead of calculating the impedance it simply uses the ratio between the input voltage and the output voltage. In Matlab the function polyfit was used to find an exponential equation that fitted the curve of the sampled values. The resulting values of the equation can be seen in tables A.3 and A.4.

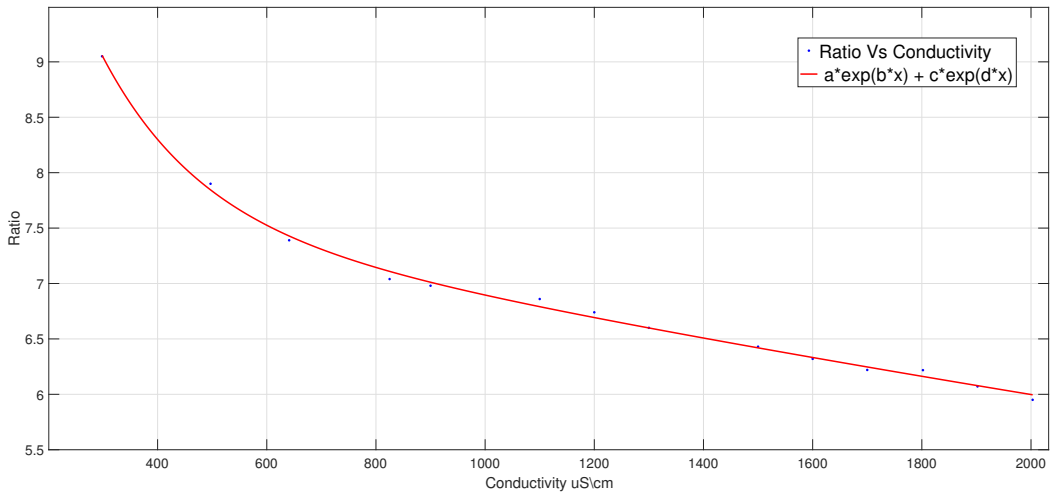

Figure 4.9: Data points matched with exponential equation.

5
Discussion and Conclusion

This final chapter provides a discussion of the outcomes. It will also outline potential interesting future work and finally present the conclusion of the thesis.

5.1 Discussion

The goal of this thesis was to design a low-cost conductivity measuring system and part of this was to design an inexpensive probe. The parallel plated probe was chosen as it is both reliable and can be manufactured at a low cost. The printed circuit board (PCB) consists of a copper plate on top of fibreglass laminate, which makes the material cost low. In addition to the low material cost there also exists several PCB manufacturers, which means that the cost of the probe can be further decreased. The only additional assembly after the PCB manufacturing process is the attachment of the probe's contacts to the control board making the after assembly minimal.

The parallel plated probe compared to side plated probes and finger plated probes, makes up for the additional space it occupies with an additional PCB by having better protection from being short circuited compared with similar PCB based conductivity probes that only utilize one PCB. The tank is repeatedly being filled with water and emptied in cycles. As this process goes on, salt from the water will eventually start to grow on the surface of the PCB. This will eventually lead to a bridge being formed between the two probes on the plate causing a short circuit. By using two plates, this problem is partially avoided as the only physical connection between the probes is the liquid. There might still be some growth of salt on the probes which will add an offset to the conductivity being measured as the surface of the probe is contaminated with detergent.

The dimensions of the plates were chosen to make the capacitance of the probe large enough to be able to theoretically neglect the other capacitance than C_{ox}. As mentioned, the capacitance can in theory be neglected when the capacitance of the surface oxide is an order of magnitude higher. The effect that the salt has on the probe will also depend on the size of the probe, as a larger probe will have a larger surface area and therefor be less sensitive.

In this thesis, water with a conductivity in the range between 100-2000 μS/cm was measured. To measure this conductivity an op-amp in a transimpedance amplifier configuration was used. The reason for this is that a constant voltage source gives a higher resolution in this specific range of conductivity. If higher values of conductivity are being measured it might be better to use a constant current source instead. A constant current setup should give higher resolution for higher values of conductivity. The conversion between constant voltage and current source can be done by changing the configuration of the op-amp.

In this study the resistor placed in series with the probe is not the optimal value. The resistor is used to guarantee that the total measured impedance never falls below the value of feedback resistor, for the transimpedance amplifier. The series resistor value should be zero as the feedback resistor should be equal to the lowest impedance value that the probe can become. However, the lowest impedance value for the probe in this specific range of conductivity is not exactly known. The problem can be fixed by performing more measurements to find a better fitting feedback resistor or at least a lower valued series resistor.

At first the aim of this study was to identify and calculate the individual components of the estimated Randles circuit presented in the method chapter. To be able to measure conductivity, the ratio between the input signal and the output signal was measured. The input signal was then divided by the value of the feedback resistor to obtain the calculated impedance. As can be seen from the results there is a mismatch between the estimated and the measured values. To solve this problem a simpler method was used: that of fitting a mathematical model to the measured values. The module equation is then used to convert the measured impedance into conductivity. This method does however lack physical explanation between the measured values and conductivity. In theory only the input voltage needs to be measured. However, the output voltage cannot be guaranteed to be stable and therefore there is a benefit to measure the output voltage.

Something that was not planned from the beginning but became clear while testing the probe, was that it might be possible to measure with the probe outside the tank. This is because as the tank is made of plastic and it is clear that the AC signal does not seem to have a problem traveling through plastic. This would protect the probes from being coated in salt by the liquid which would significantly increase the lifespan of the probes. While testing the probe it became clear that a change in water level reflected a linear change in impedance. This would in theory mean that the probe potentially would also work as a water level meter.

5.2 Future Work

From the previous section it can be deduced that there exist several possible improvements to the design, which could have been made with more time and resources. A software improvement would be to compensate for temperature variations in the liquid. As mentioned in the theory section, conductivity is sensitive to temperature variations and a change in temperature between readings can cause the system to assume a wrong value. Therefore, it is important to compensate for the temperature variation. For this reason the system was designed with the possibility of using a standard one-wire protocol temperature probe. When the temperature is known the variation in conductivity can then be compensated by using algorithms as mentioned in the theory chapter. Another software improvement would be to increase the FFT sample size as this would increase the resolution of the system. An evaluation would have to be made if the benefit of increased resolution outweighs the downside of increased measurement time. To further reduce errors, an average over several measurements could be taken, which would reduce the effect that interference has on readings.

The size of the probe can be further optimized for the existing system design. The benefit of reducing the size of the probe is that it is easier to fit the probe into smaller volumes. However there is a direct limitation with the range of impedance the current system can measure. This limitation is the maximum change in impedance the ADCs can measure, another problem is when the size of the probe is reduced. At a certain point it will no longer be possible not to account for other capacitances. Further work would include finding the optimal balance between the size and the system, alternatively to add external ADCs with higher resolution.

As mentioned in the discussion the probe consists of a printed circuit board which is made of fiberglass laminate. The copper plate that is glued to the fiberglass is covered in a thin layer of epoxy laminate. The thin layer of laminate that shields the copper plate from the liquid must withstand being submerged in the liquid for years. A long-term study to determine the water's effect on the degeneration of the laminate could be conducted using various thickness of epoxy laminate. There is a possibility to avoid this degeneration of the probe by placing the probe outside the plastic tank. By placing the probe directly against the plastic of the tank with the copper part facing towards the water in the tank it is possible to detect a change in the measured impedance. That would mean that it might be possible to have the probe mounted on the outside the tank.

Further tests to see how well it works with measuring the conductivity of the liquid from the outside of the tank needs to be done. If this works, it would mean that the probe would not directly interact with the liquid that is being measured and, in that way, not be affected or effect the water that is being measured. This might even reduce the effect that salt has on the probe as the probe no longer stands out from the wall of the tank or interferes with the flow of water that happens when the tank is filled and emptied.

Further investigation in to a potential other application for the conductivity meter is as a water level meter. As previously mentioned, there is a noticeable linear change in the impedance as the water level varies against the copper plated area of the probe. The variation is particular noticeable as the air does not conduct electricity very well and the impedance would rise with the decrease of the water level in the tank.

5.3 Conclusion

In this thesis a low-cost system for measuring conductivity in greywater is presented and evaluated. Microcontroller and a parallel plated conductivity probe is used to measure the conductivity of the liquid. The probe is made of epoxy laminate and copper in the same way as a standard printed circuit board. Because of the low material cost and several available vendors, the probe can be manufactured at a low cost. The simplicity of the design of the probe makes it so the size of the probe can be modified to better fit in other designs. The system is developed for measuring conductivity in the range between 100-2000 uS/cm and the resolution of the conductivity meter is limited to the resolution of the analog digital converter and the accuracy of the transimpedance-amplifiers feedback-resistor.

For higher values of conductivity, the configuration of the operational amplifier can be modified to be a constant current source. The system uses AC-signals which can pass through the plastic film on the PCB. Further studies can be conducted to investigate the possibility of measuring conductivity through thick acrylic plastic, protecting the probe from the corrosive liquid.

References

[1] Mimbly company website. https://mimbly.net/. Accessed: 2018-01-15.

[2] Stmicroelectronics : Stm32f303xc. http://www.st.com/en/microcontrollers/stm32f303rc.html. Accessed: 2018-01-15.

[3] Kfriedrich wilhelm georg kohlrausch. https://www.britannica.com/biography/Friedrich-Wilhelm-Georg-Kohlrausch. Accessed: 2018-10-02.

[4] N. Kumar. *Comprehensive Physics XII.* Laxmi Publications, 2004.

[5] Masaki Hayashi. Temperature-electrical conductivity relation of water for environmental monitoring and geophysical data inversion. *Environmental Monitoring and Assessment*, 96(1):119–128, Aug 2004.

[6] S. Hu, K. Wu, H. Wang, and J. Chen. Electrical conductivity measurement method in seawater desalination based on variable frequency excitation. In *2009 9th International Conference on Electronic Measurement Instruments*, pages 1–810–1–813, Aug 2009.

[7] Freek Brinkmann, Niels Ebbe Dam, Francesca Deák, Eva andDurbiano, Enzo Ferrara, Judit Fuko, Hans Jensen, Michal Mariassy, Rubina H. Shreiner, Petra Spitzer, Uwe Sudmeier, Michael Surdu, and Leoš. Vyskocil. Primary methods for the measurement of electrolytic conductivity. *Accreditation and Quality Assurance*, pages 346–353, 2003.

[8] Shanzhi Xu, Peng Wang, and Yonggui Dong. Measuring electrolyte impedance and noise simultaneously by triangular waveform voltage and principal component analysis. *Sensors*, 16:576, 04 2016.

[9] W. Olthuis, W. Streekstra, and P. Bergveld. Theoretical and experimental determination of cell constants of planar-interdigitated electrolyte conductivity sensors. *Sensors and Actuators B: Chemical*, 24(1):252 – 256, 1995.

[10] Parra Lorena, Sendra Sandra, Ortuno Vicente, and Jaime Lloret. Low-cost conductivity sensor based on two coils. *Recent Advances in Intelligent Control, Modelling and Computational Science*, pages 141–144, August 2003.

[11] K. Striggow and R. Dankert. The exact theory of inductive conductivity sensors for oceanographic application. *IEEE Journal of Oceanic Engineering*, 10(2):175–179, Apr 1985.

[12] R. N. Dean, A. K. Rane, M. E. Baginski, J. Richard, Z. Hartzog, and D. J. Elton. A capacitive fringing field sensor design for moisture measurement based on printed circuit board technology. *IEEE Transactions on Instrumentation and Measurement*, 61(4):1105–1112, April 2012.

[13] P. Boškoski et al. *Fast Electrochemical Impedance Spectroscopy: As a Statistical Condition Monitoring Tool.* Springer International Publishing, 2017.

[14] Evgenij Barsoukov and J. Ross Macdonald. *Impedance Spectroscopy : Theory, Experiment, and Applications*. John Wiley & Sons, Incorporated, 2005.

[15] P. Boškoski et al. *Fast Electrochemical Impedance Spectroscopy: As a Statistical Condition Monitoring Tool.* Springer International Publishing, 2017.

[16] Andrzej Lasia. *Electrochemical Impedance Spectroscopy and Its Applications*, volume 32. Springer-Verlag New York, 01 1999.

[17] Asif I. Zia and S.C. Mukhopadhyay. *Electrochemical Sensing: Carcinogens in Beverages*, volume 20. Springer-Verlag New York, 01 2016.

[18] J. E. B. Randles. Kinetics of rapid electrode reactions. *Discuss. Faraday Soc.*, 1:11–19, 1947.

[19] Andrzej Lasia. *Electrochemical Impedance Spectroscopy and Its Applications*, volume 32. Springer-Verlag New York, 01 1999.

[20] S. M. M. Alavi, A. Mahdi, S. J. Payne, and D. A. Howey. Identifiability of generalized randles circuit models. *IEEE Transactions on Control Systems Technology*, 25(6):2112–2120, Nov 2017.

[21] W. Olthuis, A. Volanschi, J.G. Bomer, and P. Bergveld. A new probe for measuring electrolytic conductance. *Sensors and Actuators B: Chemical*, 13(1):230 – 233, 1993.

[22] Atlas scientific : E.c. probe k 1.0 webpage. `https://www.atlas-scientific.com/product_pages/probes/ec_k1-0.html`. Accessed: 2018-01-15.

[23] Atlas scientific : E.c. probe k 1.0. `https://www.atlas-scientific.com/_files/_datasheets/_probe/EC_K_1.0_probe.pdf`. Accessed: 2018-01-15.

[24] Atlas scientific embedded conductivity circuit. `https://www.atlas-scientific.com/_files/_datasheets/_oem/EC_oem_datasheet.pdf`. Accessed: 2018-01-15.

[25] Datasheet, ds18b20. `http://www.st.com/content/ccc/resource/technical/document/datasheet/f2/1f/e1/41/ef/59/4d/50/DM00058181.pdf/files/DM00058181.pdf/jcr:content/translations/en.DM00058181.pdf`. Accessed: 2018-01-30.

[26] An3116 application note stm32$^{TM's}$ adc modes and their applications. `http://www.st.com/content/ccc/resource/technical/document/application_note/c4/63/a9/f4/ae/f2/48/5d/CD00258017.pdf/files/CD00258017.pdf/jcr:content/translations/en.CD00258017.pdf`. Accessed: 2018-02-20.

[27] An2834 application note how to get the best adc accuracy in stm32 microcontrollers. `http://www.st.com/content/ccc/resource/technical/document/application_note/group0/3f/4c/a4/82/bd/63/4e/92/CD00211314/files/CD00211314.pdf/jcr:content/translations/en.CD00211314.pdf`. Accessed: 2018-02-20.

[28] Thickness of solder resist on fr4 board. `https://www.pcbway.com/blog/Engineering_Technical/PCB_design__fabrication.html`. Accessed: 2018-02-01.

[29] C. G . Malmberg and A. A. Maryott. Dielectric constant of water from 00 to 1000 c. *Research of the National Bureau of Standards*, 56(January 1), 1956.

[30] Ne5534x,sa5534xlow-noise,operational amplifiers. `http://www.ti.com/lit/ds/slos070d/slos070d.pdf`. Accessed: 2018-04-20.

[31] Ltspice iv webpage. https://www.analog.com/en/design-center/design-tools-and-calculators.html. Accessed: 2018-01-15.
[32] Stmicroelectronics :stm32cubemx. http://www.st.com/en/development-tools/stm32cubemx.html. Accessed: 2018-01-15.
[33] ac6-tools. http://www.ac6-tools.com/. Accessed: 2018-01-15.
[34] Cmsis dsp software library. http://www.keil.com/pack/doc/CMSIS/DSP/html/index.html. Accessed: 2018-04-30.

A

Appendix 1

A.1 General Information

A.1.1 Test Board Component list

The components used to make the test board.

Name	Value	Amount
STM32F303xC	N/A	1
Connector Terminal_Block1x03_5mm	N/A	1
JTAG 20 pin	N/A	1
Resistor_0805	0Ω	1
Resistor_0805	10KΩ	1
Resistor_0805	500Ω	3
Capacitor_0805	100nF	7
Capacitor_0805	1μF	2
Capacitor_0805	22μF,4.7μF	1
Capacitor_0805	1pF	2
LED_0805	N/A	1
Pin_Header_Angled_1x04_Pitch2.54mm	N/A	1
USB_Mini-B	N/A	1
Pin_Header_Straight_2x10_Pitch2.54mm	N/A	1
Jumper_2Pin_SMD	N/A	2
LDO_TS2940CW−3.3	N/A	1

Table A.1: Component list of the Test board

A.1.2 ARM MCU STM32F303xC Connections

The following table show the Pin setup.

Pin Function	Pin Name	Pin Number
ADC2_IN2	PF4	18
DAC1_OUT	PA4	20
ADC4_IN3	PB12	34
ADC3_IN5	PB12	33
SWIDO	PA13	46
SWD_CLK	PA14	49
SWO	PB3	55
T_rest	PB4	56
Boot0	BOOT0	60
nRest	NRST	7
GPIO	PC0	8
VDD	PC14,VDDA,VDD,	2,13,19,32,46,64
GND	GND,VSS	12,31,47,63

Table A.2: Test board pin setup, an overview of STM32F303xC pin-out can be seen in datasheet [25]

A.1.3 General Setup Information

The board was programmed in C using STM32CUBEMX [32] and the HAL library, the editor was ac6 [33]. All the software was made using commercial licenses and should be legal to commercially distribute. ST Microelectronics has released STM32CUBEMX as a tool to quickly configure basic MCU functions, like timers and ADC. The STM32F303 also offers internal op-amps which can be configured using CUBEMX CMSIS [34].

A.2 Schematics

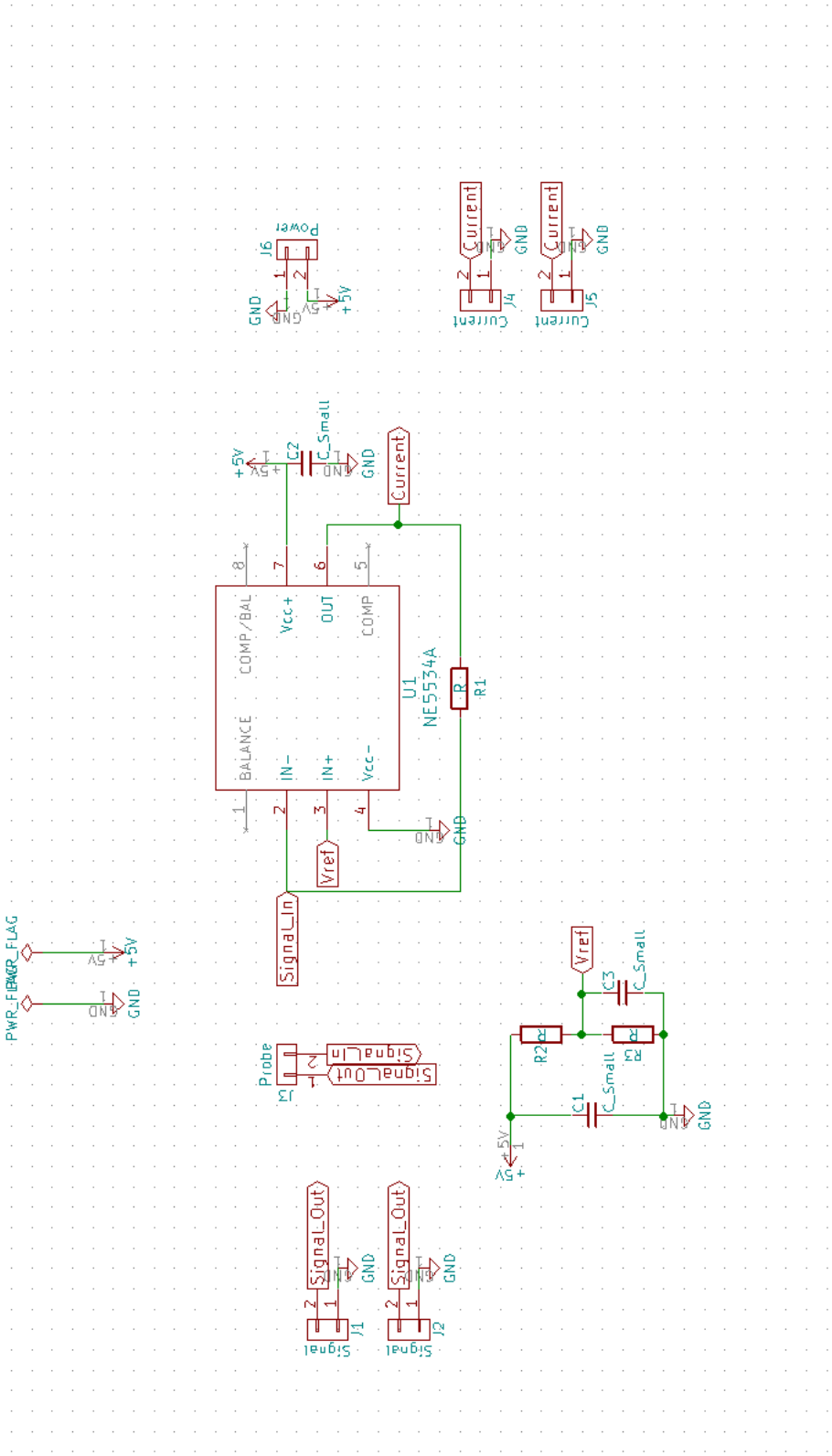

Figure A.1: Schematic of the breakout board

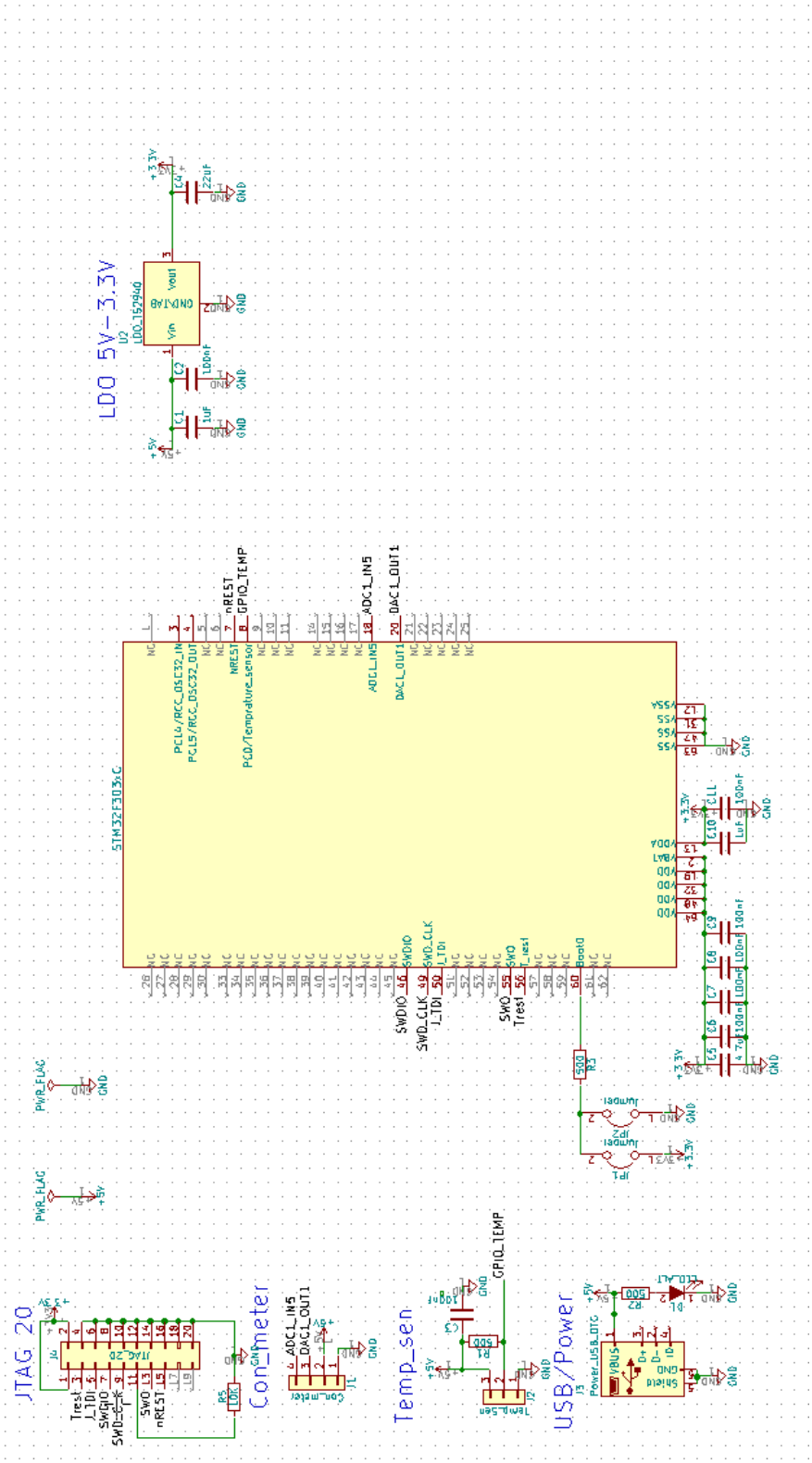

Figure A.2: Schematic of the Circuit

A.3 Probe Test Setup

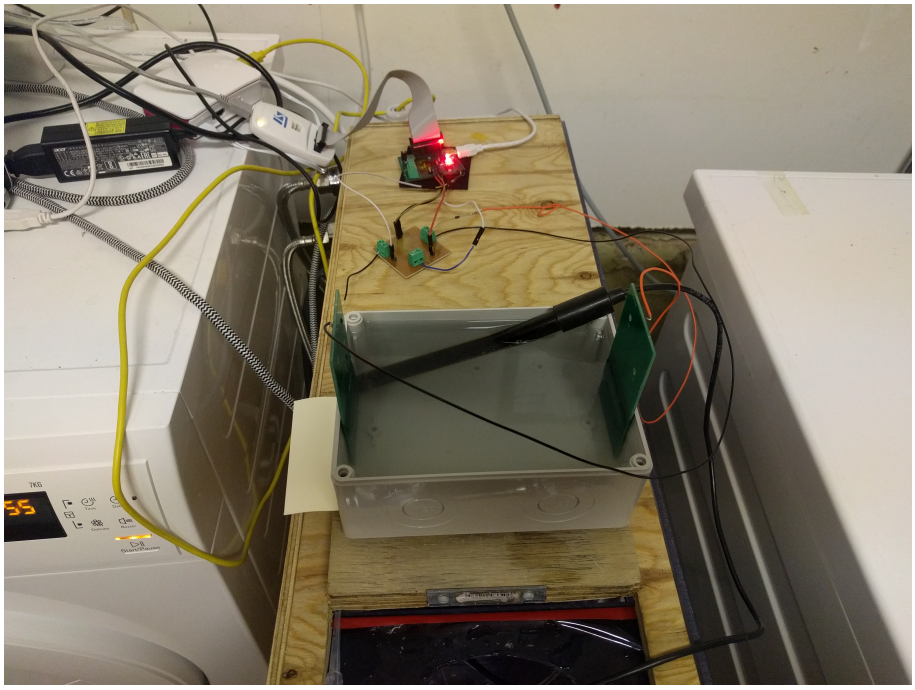

Figure A.3: Test setup figure 2

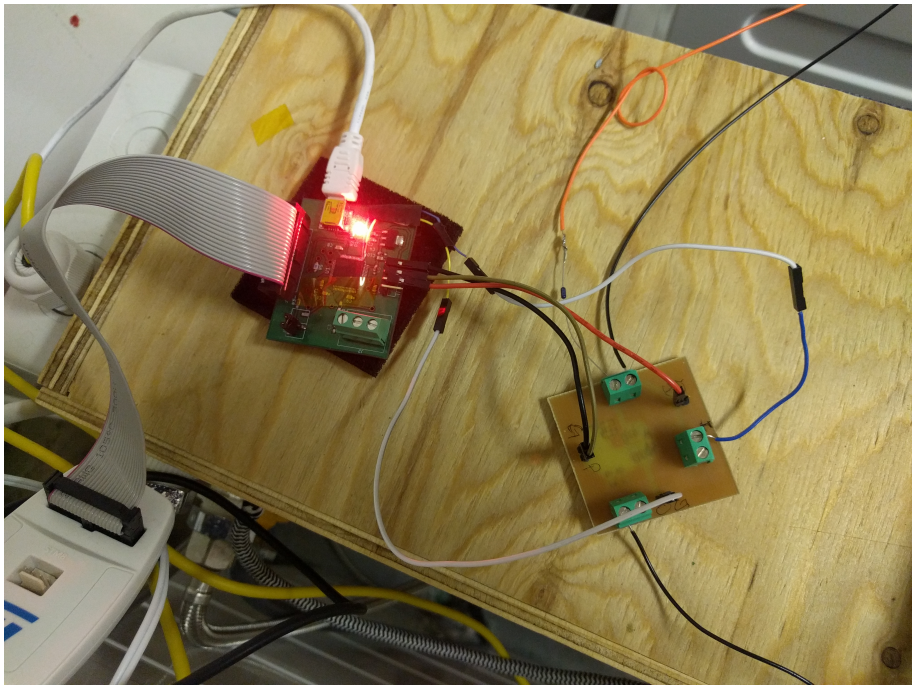

Figure A.4: Test setup figure 1

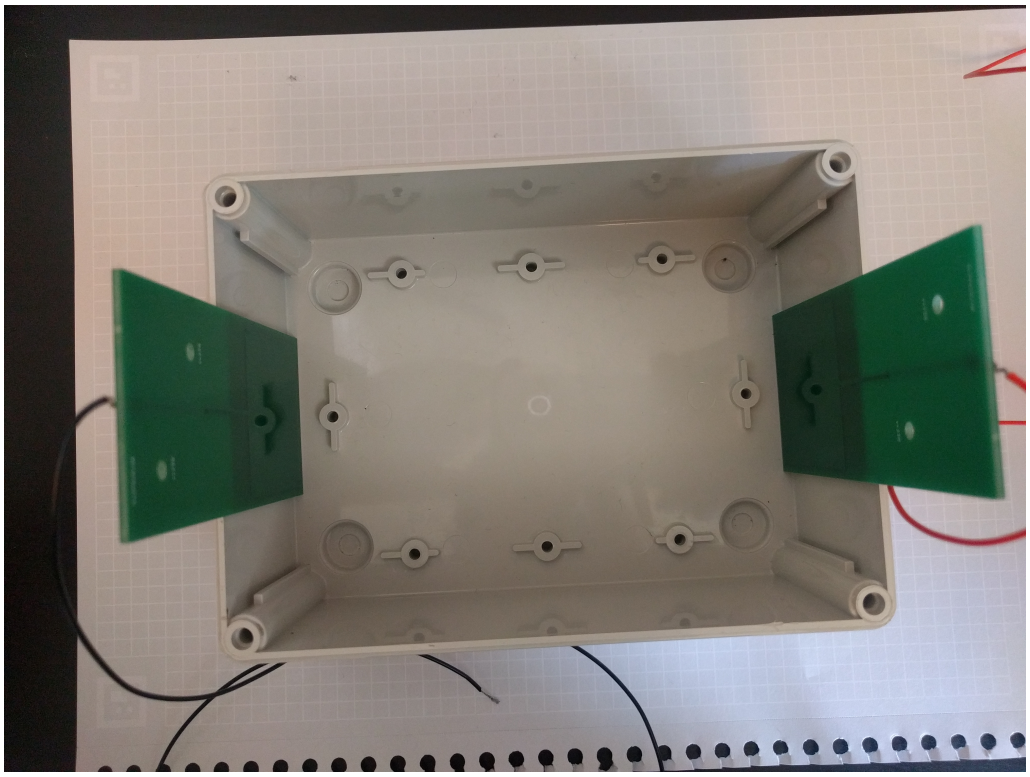

Figure A.5: Actual probe in setup

A.4 Results

The equation used to estimate the measured curve in figure 4.9. The table A.3 shows the deviation from the mean estimated values of the function and table A.4 shows the fitness of the function to the measured curve.

$$f(x) = a * exp(b * x) + c * exp(d * x) \tag{A.1}$$

Table A.3: Constants to the equation f(x) = a*exp(b*x) + c*exp(d*x)

	Mean	Min	Max
a	8.037	4.785	11.29
b	-0.005606	-0.007183	-0.004029
c	7.86	7.636	8.084
d	-0.0001352	-0.0001533,	-0.000117

Table A.4: The equation's fitness values

SSE:	0.02377
R-square:	0.9974
Adjusted R-square:	0.9966
RMSE:	0.04875